

# **A comparative study on hole quality criteria in CFRP drilling**

**Jerome Paul Raenius Sakthivel  
Balaji**

**2021**

LUTMDN/(TMMV-5314)/1-53/2021



**LTH**  
FACULTY OF  
ENGINEERING

---

MASTER THESIS  
DIVISION OF PRODUCTION AND MATERIALS ENGINEERING  
LUND UNIVERSITY

Supervisor:

Andrii Hrechuk, PhD, Production and Materials Engineering, Lund University

Examiner:

Jan-Eric Ståhl, Professor, Production and Materials Engineering, Lund University

Authors: Sakthivel Balaji & Jerome Paul Raenius Jeevanandham  
Lund, Sweden 2021

Division of Production and Materials Engineering  
LTH, School of Engineering  
Lund University  
Box 118  
SE-221 00 Lund  
Sweden

---

## Foreword

We present the master thesis “A comparative study of hole quality criteria in CFRP drilling”, based on the analysis work carried out in LTH during the time January – May 2021. The authors are indebted for the opportunity provided to collaborate with the division of Production and Materials Engineering. The authors are grateful and thankful to all the faculties in LTH. We take this opportunity to thank all the personnel and highlight some key contributions.

Firstly, we would like to praise and thank God, the Almighty, who has granted us countless blessings, knowledge, and opportunity to the authors, so that we have been finally able to accomplish the thesis.

Dr. Andrii Hrechuk, we heartily thank you for your excellent guidance and continuous support during this process. You always spent time with us to discuss the challenges and provided meaningful insights which helped us throughout the process and gave us solutions. We thank you for the trust that you have bestowed upon us and for your timely advice at each step of the process. Your enthusiasm and feedback in the weekly meetings motivated us throughout the work. It was truly an honor working under your guidance and learn all we could about carbon fiber.

We would also like to thank Dr. Volodymyr Bushlya, Dr. Christina Windmark and Professor Jinming Zhou at Lund University for their valuable input and investing their precious time in making this project successful. We would also like to thank our parents, for their support and guidance throughout our studies. Last, but not least, we would like to extend our sincere thanks to our fellow classmates at LTH for their constant support and love throughout this journey.

Jerome Paul Raenius and Sakthivel Balaji  
2021

---

---

## Abstract

Drilling is an essential hole-making operation in the modern industrial world. Drilling operation is comparatively challenging in composites when compared to metals. Composites are heterogeneous and possess a high strength-to-weight ratio which makes it a challenge in composite drilling. The hole quality has two major defects affecting the reliability of CFRP composites: Uncut fibers and Delamination are critical factors responsible for gap formation, leading to loosening and slacking of the joints. This Phenomenon has a high degree of risk in the reliability of joints. The drilling process of CFRP can be optimized using optimum tool geometry and cutting data. This thesis analyzes hole quality factors such as the Delamination and uncut fibers, aiming to find an optimum tool geometry for minimal tool wear. This thesis aims to identify the key parameters which influence the formation of undesirable defects found in drilling composites. These hole quality effects result negatively in bolted and riveted connection between CFRP Components which is a significant safety concern in the Aerospace and Motorsports field.

During the initial phase, extensive research has been carried to gather data through literature surveys. This research was responsible for understanding the tool geometry influencing the defects such as Delamination or uncut fibers, which has set a foundation for the experimentation. The second phase entails analyzing CFRP specimens using Alicona Infinite focus. Whereas, in the final stage, the data from the microscopic images are processed using MATLAB scripts to calculate and compare the delamination factor and uncut fibers under varying cutting conditions and tools.

The results are plotted using graphs to compare delamination and uncut fiber under varying cutting and tool coatings. The reason for the hole quality behavior has been discussed briefly in the later chapter.

**Keywords:** CFRP, Composites, Hole quality, Delamination, Uncut fibers

---

---

# TABLE OF CONTENTS

<b>1. Introduction</b>	<b>1</b>
1.1. Condition for thesis	1
1.2. Purpose	1
1.3. Problem description	1
1.4. Limitations	2
<b>2. Theory</b>	<b>3</b>
2.1. Background	3
2.2. Production methodology	4
2.3. Machinability of carbon fiber	5
2.4. Tool geometry	6
2.5. Hole Quality	7
2.6. Defect evaluation	10
2.7. Tool wear	13
<b>3. Methods and materials</b>	<b>15</b>
3.1. Workpiece material	15
3.2. Tools used	15
3.3. Drilling Process	15
3.4. Method of analysis	16
3.5. Microscopy	16
3.6. Overall analysis algorithm	17
3.7. Determination of hole diameter	20
3.8. Pre-processing before determination of uncut fibers and delamination	20
3.9. Processing profiles of delamination and uncut fibers	21
<b>4. Results</b>	<b>22</b>
4.1. Prerequisites of the drilling tests	22
4.2. Analysis of delamination	23
4.3. Analysis of uncut fiber area	36
<b>5. Discussion and Conclusion</b>	<b>40</b>
<b>6. References</b>	<b>43</b>
<b>7. APPENDIX</b>	<b>46</b>

---

---

## TABLE OF FIGURES

Figure 1. a) A schematic representation of Unidirectional laminates b) A schematic representation of Quasi-isotropic laminates [19].....	6
Figure 2. Cutting geometry of a drill [20].....	7
Figure 3: (a) Drilled hole of a CFRP panel; (b) Delaminated area of the drilled hole .....	9
Figure 4. Schematic representation of Area and Diameter of delamination[1].....	11
Figure 5. Representation of equivalent delamination factor ( $F_{ed}$ ) [1].....	12
Figure 6. Drilled CFRP panel placed under Alicona.....	17
Figure 7: Different steps involved in determination of hole sequence for analysis	18
Figure 8: Schematic representation of Image processing sequence determination	19
Figure 9. Algorithm for defining the contours of uncut fibers and delamination...	21
Figure 10: Comparison of Delamination area for different cutting data a) $vc=100$ mm/rev; $f=0.02$ mm/rev b) $vc=100$ m/min; $f=0.05$ mm/rev c) $vc=100$ m/min; $f=0.15$ mm/rev d) $vc=100$ m/min; $f=0.1$ mm/rev e) $vc=140$ m/min; $f=0.02$ mm/rev f) $vc=140$ m/min; $f=0.1$ mm/rev g) $vc=180$ m/min; $f=0.05$ mm/rev h) $vc=180$ m/min; $f=0.15$ mm/rev .....	25
Figure 11. Drilled holes using cemented carbide drill with $vc$ 100 m/min, $f$ 0.02 mm/rev, (a) the 1 <sup>st</sup> drilled hole and (b) is 160 <sup>th</sup> drilled holes, (c,d) are holes with recognized delamination contours .....	27
Figure 12: Comparison chart of delamination area for all cutting data.....	28
Figure 13: Slope values for each cutting data .....	29
Figure 14: Delamination factors for different cutting data; a) $vc=100$ m/min; $f=0.02$ mm/rev b) $vc=100$ m/min; $f=0.05$ mm/rev c) $vc=100$ m/min; $f=0.15$ mm/rev d) $vc=100$ m/min; $f=0.1$ mm/rev e) $vc=140$ m/min; $f=0.02$ mm/rev f) $vc=140$ m/min; $f=0.1$ mm/rev g) $vc=180$ m/min; $f=0.05$ mm/rev h) $vc=180$ m/min; $f=0.15$ mm/rev.....	30
Figure 15: Comparison chart for delamination factor $F_d$ .....	32
Figure 16: Comparison chart for adjusted delamination factor, $F_{da}$ .....	33
Figure 17: Comparison chart for Equivalent delamination factor $F_{ed}$ .....	34
Figure 18: Delamination area for PCD coated tool.....	35
Figure 19: Delamination factor chart for PCD coated tool .....	35
Figure 20: Combined chart for uncut fiber area for different cutting data a) $vc=100$ m/min; $f=0.02$ mm/rev b) $vc=100$ m/min; $f=0.05$ mm/rev c) $vc=100$ m/min; $f=0.15$ mm/rev d) $vc=100$ m/min; $f=0.1$ mm/rev e) $vc=140$ m/min; $f=0.02$ mm/rev f) $vc=140$ m/min; $f=0.1$ mm/rev g) $vc=180$ m/min; $f=0.05$ mm/rev h) $vc=180$ m/min; $f=0.15$ mm/rev .....	36
Figure 21: Comparison chart for uncut fiber area .....	38
Figure 22: Uncut fiber area chart for PCD drill .....	39

---

---

## TABLE OF SYMBOLS

<i>Symbol</i>	<i>Description</i>	<i>Unit</i>
$F_d$	Delamination factor	[-]
$F_{da}$	Adjusted delamination factor	[-]
$F_{ed}$	Equivalent delamination factor	[-]
$D_{max}$	Maximum delamination diameter	[mm]
$D_{nom}$	Nominal hole diameter	[mm]
$A_d$	Delamination area	[mm <sup>2</sup> ]
$A_{nom}$	Nominal hole area	[mm <sup>2</sup> ]
$D_e$	Equivalent delamination diameter	[mm]
$D_f$	Delamination area factor	[mm <sup>2</sup> ]
$A_{max}$	Maximum delamination area	[mm <sup>2</sup> ]
CFRP	Carbon fiber reinforcement polymer	[-]
vc	Cutting speed	[m/min]
f	Feed rate	[mm/rev]

## LIST OF TABLES

Table 1: Cutting data used.....	22
Table 2: Sample data.....	23

---

---

# 1. Introduction

This chapter entails the introduction of thesis with a brief insight of the work done, a brief explanation on the approach of the thesis, the conditions that are required for the thesis, the purpose of the thesis, a brief description of the topic and the limitations that the thesis contains.

## 1.1. Condition for thesis

This Master thesis comprises 30 hp credits, is a part of the Department of Production and Materials Engineering at the Faculty of Engineering, Lund University. The Project details the influence of hole quality during CFRP drilling affecting their reliability of CFRP components. Resources for testing, analyses, and writing are provided by the Department of Production and materials engineering, LTH.

## 1.2. Purpose

This thesis aims to explain the impact of the hole quality aspects during CFRP drilling. This study entails analyzing hole quality defects such as delamination and uncut fibers of drilled holes in CFRP parts, including the comparison of two different cutting tools and multiple cutting data. It also includes the in-depth analysis of the hole quality criteria, which can be used for the evaluation of defect size, and the relationship between these criteria. The outcome is aimed to achieve the knowledge regarding the defect formation and quality criteria which can further be implemented for evaluation of the product quality in the industrial scale.

## 1.3. Problem description

Drilling is an essential hole-making operation in the manufacturing field. In the case of composites, high strength ratio (4.5 GPa above), abrasive properties lead to intensive tool degradation and make it challenging to achieve tolerance in the hole-making process [1]. However, tolerance is a crucial factor in manufacturing and assembling a product. Formation of hole defects such as **delamination** and **uncut fibers** were considered critical factors influencing the tolerance levels of the machined CFRP components. CFRP has been widely used in Aerospace, Motorsports, and sports equipment. The formation of delamination and uncut fibers in CFRP components leads to a gap in a joint bolt or rivet connection. This gap leads to loosening and slacking of the joints in CFRP components, which negatively impacts the reliability of these components. Especially in the



---

aerospace industry, reliability is a crucial factor because of safety concerns. It is essential to achieve the desired tolerance and hole quality to meet the high standards. Various parameters such as tool geometry, tool type, and cutting data are responsible for the hole quality and tolerance. It is necessary to study and analyze the machining parameters to avoid hole quality defects. Improvements can be made through adopting suitable tool selection and cutting data for machining.

#### **1.4. Limitations**

The primary goal of this report is to study the hole defects in CFRP using microscopy measurements to determine the relationship between the cutting data, defect formation and the tool material. The study focuses on the hole quality defects such as uncut fibers and delamination in-depth and their prevention to achieve the desired tolerance and hole quality to meet the technical needs. The understanding of the defect formation, along with its relationship with tool wear, is a key to minimize the defects. Although tool wear is a crucial part of the CFRP drilling, the impact of those will not be the main focus of the thesis. Furthermore, hole quality varies for each industrial application depending upon their technical needs.

---

## 2. Theory

The study of hole quality defect formation begins with an exploratory research in a literature survey. It also includes an explanatory research about the cause and effect of hole quality in CFRP defects such as uncut fibers and delamination. During the first phase, the quantitative data have been gathered to understand the science behind defect formation and composite drilling. Literature review will be performed on CFRP drilling, hole quality defects, uncut fibers and delamination. This is required to set up a foundation for our experimental work which is planned to be performed in the later stages of the thesis.

### 2.1. Background

The beginning of composite materials may date back to the bricks made by ancient Egyptians who used mud and straw. However, commercialization of composite materials started only in the beginning of 19th century, when cellulose fibers were used as a reinforcement for phenolic, urea, and melamine resins. A composite material is made by combining two or more different materials having distinct properties [2]. These different materials combine to give a composite material with unique properties, which do not belong to each component individually. Although, in the composite, especially its constituents (matrix and reinforcements) can be easily distinguished as they do not blend or dissolve into each other [3]. Commonly composites are just made of two components, one is the matrix or binder that surrounds and binds together the second material which can either be fibers, fragments, or particles which are called reinforcement. The greatest advantage of a composite material is its weight to strength ratio, strength-to-stiffness, anticorrosion, antimagnetic, and other. Composites also have design flexibility because it can be molded, casted, or sintered into complex shapes [4].

Advanced properties of composite material put them in the higher hierarchy in various engineering applications like engineering structures, aircraft parts, automobiles, and in different industrial applications. Glass fiber reinforced polymers (GFRP) are the most popular reinforced composites, and other composites like high-performance carbon (CFRP) and Kevlar fiber-reinforced composites (KFRP) are all having similar fabrication process. However, all these polymers vary in their machining performance because of differences in physical and mechanical properties of the matrix and reinforcement. In polymer reinforced composites, machining depends on the reinforcement characteristics like fiber orientation, fiber amount, and fiber

---

form. Being non-homogeneous materials, composites have a significant variation in machining when compared to other conventional materials. Further, the cutting mechanism of composite material varies a lot from the cutting mechanism of conventional material, which makes analyzing their machining performance difficult [3].

Machining composite material could damage the material surface due to interlaminar and intralaminar delamination, fiber exposure, fiber crack, and matrix flow. In recent days, advanced machining techniques like electrical discharge machining, ultrasonic machining [5], laser cutting [6], and water jet [7], and abrasive water jet machining [8] are used for composite machining [3], [6]–[8]. CFRP laminates are ready-to-shape manufactured using various advanced and automated technologies like autoclave or closed mold vacuum bagging. After the curing process, there are still many micro- and macro-geometrical features that must be machined mechanically. For example, in the aerospace industry, thousands of high-quality holes must be machined to assemble CFRP parts. Although, CFRP materials are difficult-to-cut materials due to their (i) anisotropic and (ii) inhomogeneous features and (iii) the abrasive wear effects of their carbon fibers on the cutting tool. Chip removal is also crucial in CFRP because of health issues and the wear effect of carbon fibers on different parts of machine tools [9]. It is possible to produce high quality holes with the help of special drilling tools (diamond coated) using optimized process parameters. But these technologies require a considerable amount of optimization time and cost. Special hole-making techniques, like helical milling, titled helical milling or wobble milling, require longer operation times because of longer tool paths. But the amount of machining required by geometrical defects and tool cost can be significantly reduced using such special hole-making techniques [3].

## **2.2. Production methodology**

Carbon fibers are produced using a high-tech manufacturing process. It begins with a starting product called polyacrylonitrile (PAN) [10]. Polyacrylonitrile is a solid in a form of white powder. It has good non-reactive properties, high stiffness, and hardness [11]. Initially, thin threads are manufactured from polyacrylonitrile, which are further wound onto a spool which is also called as the precursor. These threads are then put in the oven in the next step. They are first oxidized between 200 and 300 degrees Celsius, then carbonized between 1200 and 1800 degrees Celsius. Threads with a high carbon content and high strength are what is left. The carbon

---

fiber is wound up and ready for use after receiving surface treatment and sizing [12].

### **2.3. Machinability of carbon fiber**

The machinability of CFRP can be analyzed by using: (i) cutting force on the cutting tool and CFRP laminates, (ii) cutting torque, (iii) surface roughness of machined surface, (iv) the delamination of CFRP layers, (v) extent of uncut fibers and (vi) tool wear [13]. These parameters are influenced by the cutting data (feed rate, cutting speed), the properties of the workpiece material and tool material. The intensifying of the cutting data always leads to increasing the cutting forces, torque, and tool wear rate. At the same time, higher cutting speed allows providing better hole quality when the drilling energy is high enough to cut reinforced fibers. The composite structure is not least important. The strength and stiffness of the carbon fiber reinforced polymers and their plies are mainly dependent on the orientation of the plies. The fibers in unidirectional material will be towards a single direction, and the strength and the stiffness will be focused only on the direction of fiber. On the other hand, woven fibers, will be oriented in two different directions, so the strength and the stiffness will be concentrated in both directions of the fiber. The layers with  $0^\circ$  plies will withstand axial loads,  $+ \text{ or } - 45^\circ$  plies will withstand shear loads, and  $90^\circ$  plies will withstand side loads [4], [13]–[15]. Composite materials are difficult to machine because of their heterogeneous structure. Conventional machining techniques like turning, milling, drilling, planning, etc., are usually used for machining composites. It is a well-known fact that in an aircraft, there are more than a million holes [16]. Therefore, from the manufacturer's perspective, 40% of all machining drilling is involved during the assembly of components. But failures like fiber rupture, deformation in the drilling zone, delamination [17] are commonly encountered. Such failures have a high impact on surface quality and hole quality. Several studies indicate that the surface quality depends on tool geometry, cutting forces, and cutting parameters. Thus, correct cutting parameters are very essential during the machining of fiber-reinforced composites [18].

---

## Fiber orientation

There are two types of fiber orientation in CFRP laminates namely: Unidirectional and Quasi-isotropic laminate. In Unidirectional (UD) laminates, the fibers are arranged in mono-direction to possess very high strength and stiffness properties in only one direction. Whereas in Quasi-isotropic laminates has in-plane stiffness in either direction due to the stacking of UD plies in various orientations such as 0, +45, -45, and 90 [19].

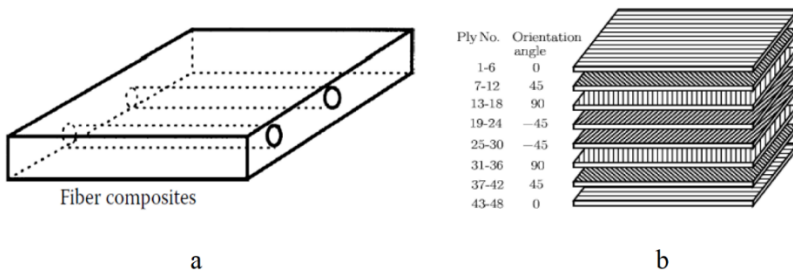


**Figure 1.** a) A schematic representation of Unidirectional laminates b) A schematic representation of Quasi-isotropic laminates [19].

Since delamination occurs on the last ply of the laminate, studies shows that there was only a slight difference in drilling between UD or quasi-isotropic composite fiber orientation. Regarding uncut fibers, the fiber orientation of composites is responsible for the direction of the uncut fiber formation. For example, if the fiber orientation of a ply is  $45^\circ$ , then the uncut fiber will be formed at an angular position of  $45^\circ$ .

## 2.4. Tool geometry

Apart from core drills and dagger drills, twist drill keeps being the most used drill bit. Despite the manufacturing complexity, twist drill provides high drilling tolerance and the possibility for cutting edge resharping. The drill point angle of a two-flute twist drill is formed by two leading cutting edges. Each primary cutting-edge function as a single point cutting tool. The cutting edge's lead angle is half that of the drill point angle. The flute allows the chip to pass through the cutting zone while also supplying coolant to the cutting

---

edge [1]. The major cutting edges are mainly responsible for material removal. The material removal process is also facilitated by the chisel edge, although to a lesser degree [19].

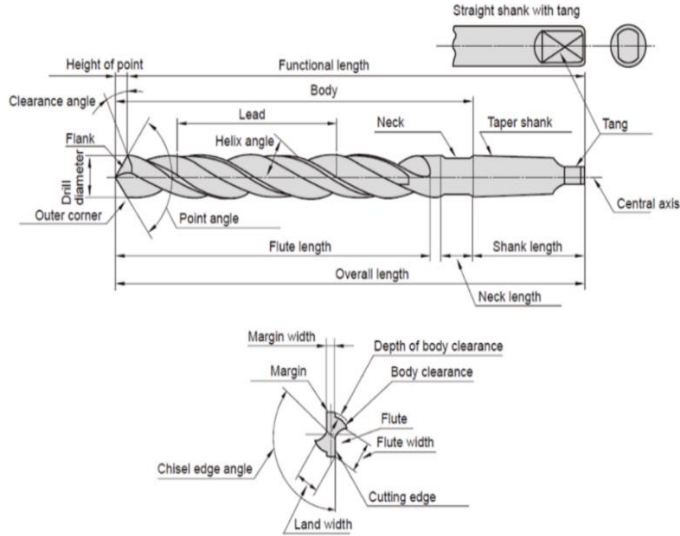


**Figure 2.** Cutting geometry of a drill [20]

The drill geometry highly influences to the cutting forces and hole quality in the result. Delamination is mainly depended on the axial cutting force because of the contact between flank drill surface and machined workpiece. Therefore, the increasing of the drill clearance angle can reduce the defect formation when drilling. At the same time, increasing the rake angle will reduce the stresses appeared on the rake face and will improve chip formation and evacuation. The cutting-edge radius is the most crucial because it effects to the formation of uncut fibers. The reducing of the cutting-edge radius allows significantly reduce the number of uncut fibers, but simultaneously, it reduces the stiffness of the cutting edge leading the breakout. The tool geometry is important part of the optimizing the CFRP drilling process and should be carefully adjusted to the entire cutting process [21].

## 2.5. Hole Quality

In composites, hole quality is major challenge in composites to thrive for because of their heterogenous nature and High strength to weight ratio. Hole

---

quality parameters include entry delamination, hole size accuracy, circularity, and surface quality. There are various ways to optimize the drilling operation in composites to achieve tolerance and high hole quality such as tool geometry, cutting data and type of cutting tool used. Process parameters can be altered such as reducing the feed, thrust force, and increasing the rotational speeds have shown significant hole quality changes in research experiments [1].

**Delamination** affects the strength of the carbon composites. Cutting tool interactions with CFRP could be complex because of its inhomogeneous and anisotropic structure. Delamination, fiber pull-out, burr, and matrix thermal degradation are being the side effects that are caused during the machining of stacks. Out of these all effects, pull-out delamination is considered as the critical one, it affects the load-carrying capacity and fatigue life drastically in a negative way. The large thrust force produced by the large point angle drills is usually responsible for the elastic deformation occurrence. Thrust force is the component of cutting force along the drill bit axis. Also, several analyses have indicated that force in the chisel edge has a significant impact than that of cutting edge [22].

The laminated layers of CFRP composite laminates can separate from each other when they are impacted by unfavorable cutting forces. This phenomenon is called delamination, which must be minimized to keep the mechanical properties of machined parts as adequate as possible. Delamination has a very huge impact on reduction strength and the fatigue life of the CFRP. Most commonly, delamination occurs due to the punch on CFRP by the chisel edge of the tool. Thrust force should be limited to avoid the delamination. Choosing proper drilling parameters to reduce thrust force is essential. However, apart from the thrust force, drilling temperature is another key factor, which can affect the properties of the composite and furtherly have an influence on delamination conditions. The thrust force significantly affects the uncut laminates during drilling process. During drilling process, the composite material takes pushing force rather than cutting force because of the lower speed of the chisel edge. Critical thrust force is inversely proportional to the drilling temperature. Delamination frequently occurs as more drilling heat gets accumulated at the exit of the hole [17], [22]–[24].

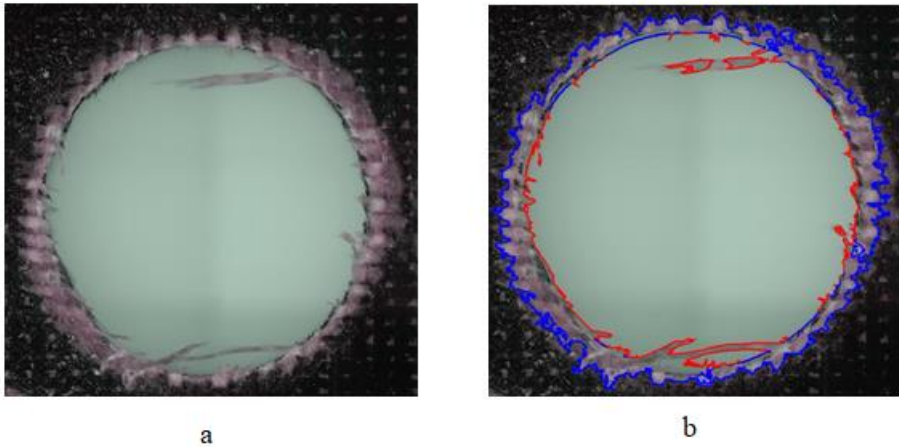


**Figure 3:** (a) Drilled hole of a CFRP panel; (b) Delaminated area of the drilled hole

*Figure 3:* (a), shows the drilled hole and the defects caused in the hole, in the drilling process. Delamination commonly take place at the exit of the hole. The captured image is focused on the exit of the hole and the delamination zone is concentrated at the circumference of the hole, as illustrated in *Figure 3:* (b). Chisel edge is a major reason for hole quality, especially delamination. Delamination occurs when the thrust force acting upon the chisel edge overcomes the interlaminar bond strength at the exit of the hole [25]. On the other hand, drilling temperature could also induce delamination [26]. Proper drilling parameters can be used to reduce thrust force. So, it is crucial to maintain critical temperature and thrust force to prevent delamination. To overcome delamination, it is effective to reduce feed rate gradually as hole exit approaches. The parameter that most affects the thrust force is the feed rate (by 90%) [26]. Although, the spindle speed is responsible only for 5 to 8% of variation of the thrust force when the machining parameters change [17], [22]–[26].

**Uncut fibers** and fiber pull-out mainly occur on the machined edges of CFRP composites when inappropriate cutting data is used. Uncut fibers usually do not negatively impact the mechanical properties of machined CFRP parts, but they necessitate additional machining operations, which increases the production time and efficiency in case their elimination is unavoidable. Uncut fibers can be removed by a deburring method. Burrs are generated mainly due to the fiber orientation angle of CFRP, the machining conditions, the tool geometry, and the tool material. A defect like



---

delamination occurs when the thrust force exceeds a critical bending moment of the fiber and polymer layers. In uncut fibers, the defect is associated with the relationship between the fiber orientation and the cutting angle. Furthermore, uncut fibers tend to increase when tool wear increases[27].

Uncut fibers are generally the first and last plies of the reinforcement fibers, which were uncut during the drilling process. Since uncut fibers, delamination, FRP thermal decomposition, hole surface damage are the major defects on CFRP drilling, the joints of the FRP material with these defects have gaps between the parts which are caused by the bending of these uncut fibers, but the parts without defects or comparatively lower level of defects fit tightly to each other [27]. Gaps create loosening and slacking of the joints in aircraft use and are unacceptable for aircraft industries for safety purposes. Thus, the evaluation of drilled hole defects plays a vital role to increase the efficiency of the aircraft assembly process and to optimize the drilling process parameters, which effectively increases the performance of aircraft.[27], [28].

## **2.6. Defect evaluation**

The aim of this segment is to do a qualitative analysis and to determine formulation of the variables that defines the hole-quality in CFRP drilling. Using the already existing research from various authors, manufacturing, and production of CFRP, composite drilling process, defects that affect the hole-quality in CFRP drilling, equations for calculating the hole-quality dependent variables are identified in this literature review. Using several research, the information to identify the length, area, and magnitude of uncut fibers and delaminated fibers were also identified. The information obtained from literature review was studied to formulate a mathematical model and method of image processing for calculating the extent of defects and hole-quality of the drilled holes.

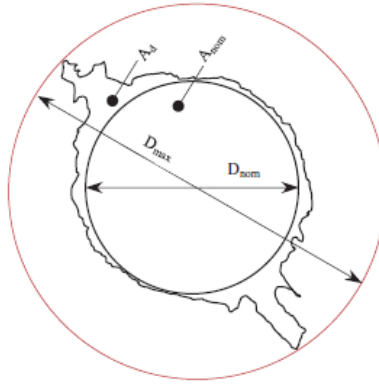


**Figure 4.** Schematic representation of Area and Diameter of delamination[1]

The defects in CFRP drilling are mainly caused because of the thrust force and improper cutting conditions used during the operation. [15]. Uncut fibers and delamination are the major defects in CFRP drilling. The findings from literature mainly focused on equations using diameter of hole, length of uncut fiber, area of delamination and uncut fiber. From several literatures, it was evident that cutting data is one of the important factor in analysing the hole quality. The spindle speed must be high, and the feed rate must be kept minimal to achieve high quality holes. But the tool life is also reduced when the spindle speed is increased, because of high temperature generated at the cutting edge during the cutting process. The delamination factor that decides the hole quality is  $F_d$  [1], which is calculated by the equation given below.

$$F_d = \frac{D_{max}}{D_{nom}}, \quad \text{Equation 1}$$

where,  $D_{max}$  is the diameter of the covering delaminated area (mm);  $D_{nom}$  is the diameter of the drilled hole (mm)

This ratio between  $D_{max}$  and  $D_{nom}$  gives the percentage of error between actual hole and delaminated hole which can also be considered as hole quality. Further, from the literature review, using image processing, the area of delamination and area of uncut fibers are identified. The ratio between area of delamination and area of hole gives the change in actual area as a factor of hole quality. This factor  $D_f$  [1] is determined using the equation given below.

---


$$D_f = \frac{A_d}{A_{nom}}, \quad \text{Equation 2}$$

where,  $A_d$  is the area of delamination ( $\text{mm}^2$ );  $A_{nom}$  is the area of drilled hole ( $\text{mm}^2$ ) is the most used delamination factor, which gives satisfactory results only when delamination possesses a pattern. However, when CFRP materials are machined, delamination presents an irregular form, containing cracks and breaks at the exit as well the entry. In these circumstances, the conventional delamination factor will not suffice because the size of the crack is not an exact representation of magnitude of the damage. Also, this factor does not determine the damage area. Thus, a novel approach is required to measure the delamination factor. This factor is called the adjusted delamination factor  $F_{da}$  [29], which is calculated using the equation given below.

$$F_{da} = F_d + \frac{A_d}{(A_{max} - A_{nom})} (F_d^2 - F_d), \quad \text{Equation 3}$$

Where,  $A_d$  is the delamination area;  $A_{nom}$ , is the drilled area of  $D_{nom}$  ( $\text{mm}^2$ );  $A_{max}$ , is the area related to  $D_{max}$  ( $\text{mm}^2$ )

The first part of the equation 3 represents the measure of the crack contribution and second part represents the damage area contribution. In this procedure, the higher the damage is on  $A_d$  has, the higher the effect on  $F_{da}$  will be. A novel approach was formulated to characterize the delamination factor  $F_d$ , called the equivalent delamination factor  $F_{ed}$  [1].

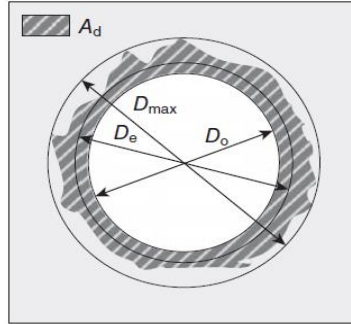


**Figure 5.** Representation of equivalent delamination factor ( $F_{ed}$ ) [1]

The scheme of the equivalent delamination factor is determined by the equation given below.

$$F_{ed} = \frac{D_e}{D_{nom}}, \quad \text{Equation 4}$$

where,  $D_e$  is the equivalent delamination diameter and can be denoted as

---

$$D_e = \left[ \frac{4(A_d + A_0)}{\pi} \right]^{0.5}$$

Equation 5

## 2.7. Tool wear

Since carbon fiber reinforced polymer is a difficult-to-machine material, tool life and machined surface quality determine machining performance. They are mainly dependent on the tool's material, cutting geometry of the tool, cutting conditions, and cutting data. Tool wear has a significant impact on drilled hole quality. The dependent variables of cutting geometry that impact the hole quality is flank wear and cutting-edge radius. The tool wear rate mainly depends on the tool material and is influenced by various material properties. The tool used for carbon fiber reinforced polymers is mainly coated and uncoated cemented carbide and diamond tools. Opposite to metallic alloys, where elastoplastic deformation occurs, much more complicated and correlated mechanisms are involved in the CFRP drilling process; this is mainly caused due to the anisotropic machinability and inhomogeneous behavior of the fiber-matrix system, which causes cutting process which is dependent on the fiber orientation and defect formation mechanisms. In a drilling operation, the tool edge segments revolve periodically and attack the fibers and matrix alternatively; This leads to an uneven distribution of cutting loads and heat generation that acts upon the tool edges during the process. The highly abrasive reinforcing fibers are subjected to abrasion and erode the shape edges of the tool while the soft matrix rubs the tool surface, which results in blunting and dulling of the drill bits[28].

**Cemented carbide** is one of the most used cutting tools in machining operations. It is denoted as WC. As the name suggests, cemented carbides are made from different carbides sintered together by a binder. Hard carbides such as tungsten carbide (WC), titanium carbide (TiC), tantalum carbide (TaC), niobium carbide (NbC) is widely used for hard metal cutting [30]. The size of the carbide particles are usually between 1-10 microns and they make up to 60 to 90 % of the Cemented Carbide [21]. The hardness, fracture toughness and heat resistance of WC can be modified according to the desired needs by varying the grain size and binder content [31]. Currently coated cemented carbide tools are used widely in machining operations such as milling, turning, and drilling. Titanium carbide (Tic), Titanium nitride (TiN), aluminium oxide- ceramic ( $Al_2O$ ) and titanium carbon nitride (TiCN) are the major coating materials used today. Chemical Vapour deposition and optimized substrate composition process together were used to coat the

---

Cemented carbide tools. Physical vapour deposition method is also used to certain extent today for the coating process.

Another tool material used for CFRP drilling is **Polycrystalline diamond (PCD)** - diamond grit that has been fused under high-pressure, high-temperature conditions in the presence of a catalytic metal. Diamond is ideal for cutting tool manufacturing due to its extreme hardness, wear resistance, and thermal conductivity. All non-ferrous materials, such as those used in the woodworking industry and chipboards, can be machined with PCD equipment [32]. In comparison to carbide, PCD is better suited to abrasive materials and has a much longer tool life. PCD is not ideal for ferrous materials due to the high solubility of carbon in iron [33].

---

## 3. Methods and materials

### 3.1. Workpiece material

A series of CFRP drilling tests were part of the current investigation's experimental phase. Drilling was performed with an EMCO PC MILL 300 with a maximum rotation speed of 10000 rpm. A KISTLER 9129AA dynamometer with a KISTLER 5070 amplifier and a National Instrument 9223 ADC has been used to measure axial force and torque during drilling. Drilling CFRP samples from the Saab AB company were used for the experimental phase of the current investigation (Sweden). It was a new type of PAN-type CFRP composite material that was used in the construction of modern Saab aircraft. A microscopy using an Alicona Infinite Focus 3D optical microscope was used to achieve structural analysis of a polished CFRP sample. CFRP samples were 4 mm thick and reinforced with a [45/90/-45/0]5s scheme. Each fiber ply is 200  $\mu\text{m}$  thick. 70 percent of the CFRP was made up of fibers with a diameter of 7  $\mu\text{m}$ . Plates measuring 70x70 mm were used to hold the samples. A unique workpiece holder was 3D printed and used. Without a substrate, it was possible to drill 26 holes in each plate [34].

### 3.2. Tools used

Drill bits made of PCD and cemented carbide were used. The Institute for Superhard Materials designed and manufactured the PCD drill bit. For comparison checking, a coated cemented carbide SECO SD203A-8.0-27-8R drill bit was used. Grinding was done on the rake and flank surfaces. As a result, this drill bit was used as a cemented carbide drill bit with no coating. Alicona Infinite Focus 3D optical microscope was used to measure the geometry [34].

### 3.3. Drilling Process

Drilling is cutting with a circular cutting motion and a geometrically determined cutting edge, with the tool's axis of revolution and the axis of the produced inner surface being the same. The feed motion follows the axes' orientation. Drillings in solid material, counterboring of existing drillings, sinking for the development of rotationally symmetrical geometries on workpiece surfaces, screwing, and rubbing to achieve high surface quality and precision are all examples of drilling applications [33].

---

### 3.4. Method of analysis

Hole quality analyses for drilled CFRP panels were performed using Alicona Infinite focus. A custom specimen holder was designed using Solidworks and 3D printed to mount the CFRP panel for microscopic measurements as shown in Figure 6. to reduce time consumption. CFRP exit surface images were taken with a 2.5x magnification optical Alicona Infinite Focus 3D microscope. 2D Images were captured to define the delamination region, uncut fiber region, and drilled hole circumference. For drilled hole image processing, special MATLAB scripts were developed.

### 3.5. Microscopy

The ability to take both profile and areal measurements with focus variation microscopy is beneficial for several surface metrology applications. Average roughness, or  $S_a$ , is defined as the mean height of a selected area and  $S_q$ , the root mean square of the mean height, and is included in the areal measurements. The calculation of  $R_a$ , which is the average roughness on a two-dimensional plane and is used in profilometry measurements, is used to calculate mean height ( $S_a$ ). The arithmetic mean of the surface texture is represented by average roughness ( $R_a$ ), with the valleys reversed to obtain a positive value. Also, on the other  $S_a$  calculates the average surface roughness in 3D. Since it is less susceptible to minor differences in surface texture, this areal measurement is useful for quantifying wear characteristics.

Alicona Infinite Focus microscope which is used in to acquire microscopic measurements in the experiments are based on the principle of focus variation. The microscope searches for the best focus related to a known distance from the sample to create a three-dimensional image. Moving the microscope objectives vertically in relation to the object, bringing the object in and out of focus, produces the image. The microscope's sensor detects and calculates where the object is in the best focus, a process that is repeated at successive lateral positions to create an image. The sensor then calculates the standard deviation of the gray levels in the local region to determine the focus by evaluating the region around each pixel. The gray values are almost similar with a low standard deviation when the focus is very low or very high. As a result, the surface topography is measured using each plane's in-focus depth, and a composite model is obtained using the in-focus slices [35].

Alicona Infinite Focus 3D is an optical 3D measurement device that is highly accurate, fast, and versatile. Users can check dimensional accuracy and calculate the surface roughness of their components with only one sensor. The number of observable surfaces is almost limitless when using Focus

---

Variation technology. Vertical surfaces are probed later using Vertical Focus Probing, an extension of Focus-Variation.

The density of measuring points is high. With up to 500 million measurement points and tolerances in the  $\mu\text{m}$  and sub- $\mu\text{m}$  ranges, as well as a broad working distance, a meticulously detailed measurement with tolerances in the m and sub-m range is ensured. Focus-high Variation's measurement point density allows operators to achieve consistent high lateral and vertical resolution across large measurement volumes. Vertical focus Probing is a pure optical measurement technology that is an extension of the Focus-Variation technology. It allows for direct measurement of surfaces with slopes greater than  $90^\circ$  and micro-holes without the need to articulate the sample [36].



*Figure 6. Drilled CFRP panel placed under Alicona*

### **3.6. Overall analysis algorithm**

The proposed methodology is based on analysis of images of the drilled holes. The methodology is mainly based on six modules that are used in a sequential order. They are: (i) defining the circumference of the hole, (ii) defining the contours of the uncut fibers, (iii) defining the delaminated area, (iv) creating and analysing the profiles of uncut fibers, (v) creating and



analysing the profiles of delamination, and (vi) estimating a general evaluation of hole quality [27].

The expected diameter, an image of the drilled hole, the scale of the image, and the measurement error are the input data. The expected diameter is normally the nominal diameter of the drill bit. This parameter is used for defining the actual hole circumference and for reducing the program runtime. Image resolution is a main factor for the accuracy of quality analysis. As the diameter of the fibers in most CFRP materials range from 7 to 15  $\mu\text{m}$ , the density of pixels in the image should be high for a better analysis[27].

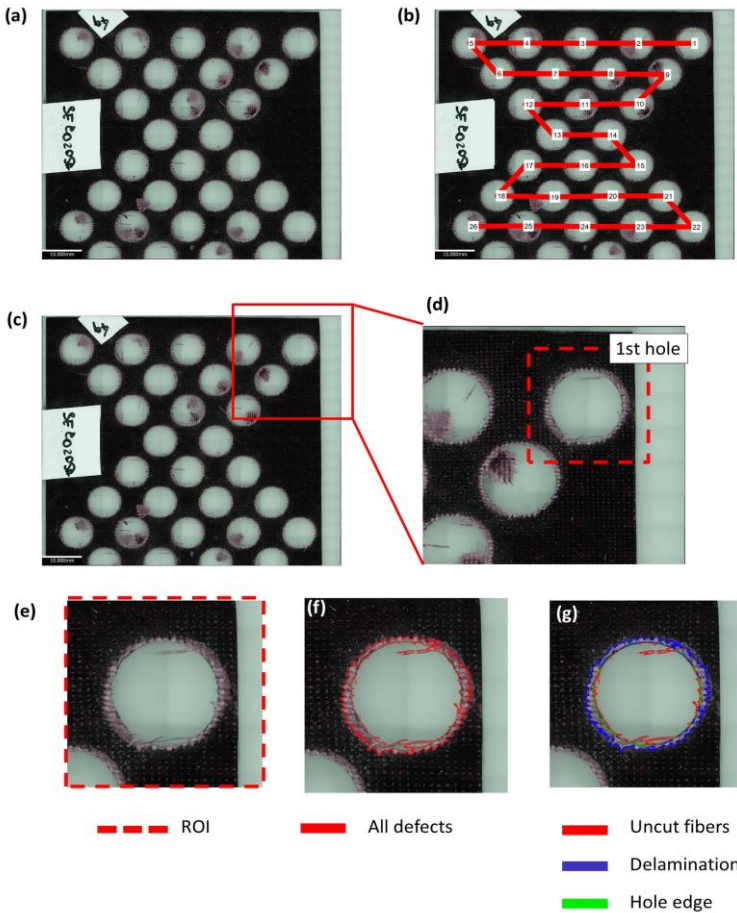


**Figure 7:** Different steps involved in determination of hole sequence for analysis

The drilled CFRP panels to be investigated were scanned under Alicona Infinite microscope by selecting points within the edges of the panels. The Drilled CFRP panel was scanned and saved in TIFF format for higher resolution, as shown in figure (a). The CNC Path for drilling holes is mapped in the scanned TIFF image as shown in (b). Then, the region of the first hole is cropped in for further analysis, as shown in (c) and (d). Then the particular region in which the selected specific hole is located is marked under the area of interest, as shown in figure (e). The specific hole defects are observed in the region of interest, as shown in figure (f). Then the hole quality defects such as uncut fibers, delamination, and hole edge were marked using red, blue, and green contours as shown in figure (g), which is used to extract values used in calculating the factors plotting the graph.

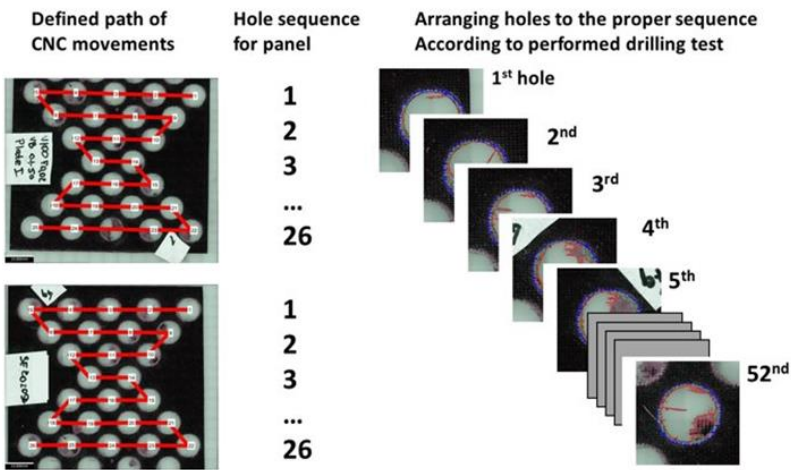


**Figure 8:** Schematic representation of Image processing sequence determination

In the above figure, the defined path of CNC movements of the drilled holes is marked in the scanned TIFF image to determine the sequence of a hole for hole quality. This mapping sequence is done to simulate and extract accurate data. According to the CNC Path, the series of the holes to be analyzed is ordered as shown in the figure. So, the first hole will have a lesser delamination area where the last 52nd hole would have a drastic difference in the delamination area.

---

### 3.7. Determination of hole diameter

The determination of the hole diameter is the initial operation of the proposed methodology. For defining the contours of the uncut fibers and delamination accurately, the actual diameter of the hole and the coordinates of the circumference must be determined precisely. The image of drilled hole, actual scale, and the expected value of diameter are the inputs for this module [27].

Defining the circle initiates with the binarization of the image by applying different contrast values and removing reflections from the image. Then, the algorithm defines the contour of the white area. The contour is created based on Moore neighborhood tracing algorithm [37]. The higher the resolution of the image, the higher the accuracy will be for analysis of contour points. But this tracing algorithm has the possibility to create duplicates of points located close to each other, which can lead to improper contour points. To overcome this issue, the Delaunay triangulation [38] method is used. Delaunay triangulation reduces the quantity of contour points and defines the outer boundary line. Delaunay triangulation method also defines and excludes the duplicates of contour points. This operation is very crucial for further steps in the process because the boundary line should only contain the points that are able to describe a circumference [27].

A special algorithm is used to identify the range of points that lies on the circumference only. This algorithm is used to define the cross-diametric pairs of points which is closest to the diameter. The least squares method [39] is used to define the coordinates of the center and the diameter of the hole from the defined pairs of points. Many defined pairs provide a reliable circumference. Now, the algorithm runs repeatedly until the actual diameter that is closest to the expected diameter is obtained [27].

### 3.8. Pre-processing before determination of uncut fibers and delamination

Defining the uncut fibers and delamination is based on their contours (Figure 9). In previous stage, the input data comprises of the actual image, the defined value of actual diameter, and the center coordinates. The data is also dependent on binarization of the image, removal of reflections, and the defining the delamination and uncut fibers. As the delamination is located at the outer rim of the hole, and the uncut fibers are located at the inner part, the areas do not belong in either locations should be excluded. The pre-

processing module neglects the outer area of the image when analyzing the uncut fibers and neglects the inner area for analyzing delamination [27].

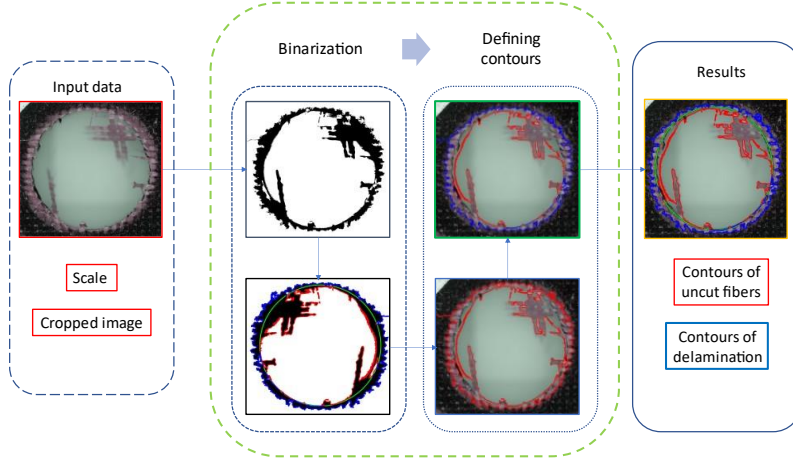


*Figure 9. Algorithm for defining the contours of uncut fibers and delamination*

### 3.9. Processing profiles of delamination and uncut fibers

By executing the previous modules, the output data obtained are diameter, center of hole, and the identified contours of delamination and uncut fibers. Using these data, parameters that define the hole quality like  $F_d$ ,  $D_f$ ,  $F_{ed}$ ,  $F_{da}$  can be identified. The data from the module provides us the hole diameter ( $D_{nom}$ ), and diameter of delamination ( $D_{max}$ ), which is substituted in [equation 1](#), which gives the delamination factor ( $F_d$ ), which is considered as the main factor that determines hole quality. The data also provides the actual hole diameter ( $A_{nom}$ ), and area of delamination ( $A_d$ ) which can be substituted in [equation 2](#), which gives the change in actual area ( $D_f$ ) as a factor of hole quality. The adjusted delamination factor ( $F_{da}$ ) is calculated using the [equation 3](#), to obtain more accurate and detailed information on damage area of the drilled hole. Further, using the values obtained from [equation 1](#) and [equation 2](#), the equivalent delamination factor ( $F_{ed}$ ) and equivalent delamination diameter ( $D_e$ ) is determined using the [equation 4](#) and [equation 5](#).

---

## 4. Results

### 4.1. Prerequisites of the drilling tests

From the information obtained from image processing, as output data from the module, results are formulated and compared for different cutting conditions in this chapter. As we have used several cutting data to perform the drilling operation, it is vital to analyze each data individually and have an overall comparison of all the data to achieve the expected results and have a clear comparison of hole quality impacting each cutting data.

*Table 1: Cutting data used*

S. No	Cutting Speed (rpm)	Feed Rate (mm/rev)	Tool used	No. of drilled holes
1	100	0.02	CC	160
2	100	0.05	CC	52
3	100	0.15	CC	74
4	100	0.1	CC	152
5	140	0.02	CC	290
6	140	0.1	CC	104
7	180	0.05	CC	76
8	180	0.15	CC	78
9	140	0.1	PCD	643
<b>Total no. of holes analysed</b>				1629

In the above table, we can see that we have used nine different cutting conditions and two different tool for the drilling operation. As CFRP is the workpiece material, several panels of CFRP material are cut at various dimensions and each hole is analyzed carefully. Nearly, 1500 holes are analyzed and all the information is compiled together for comparison to get a clear view on the hole quality criterion.

---

**Table 2: Sample data**

<b>Hole number</b>	<b>D<sub>max</sub>, mm</b>	<b>F<sub>d</sub></b>	<b>F<sub>da</sub></b>	<b>Delamination Area, mm<sup>2</sup></b>	<b>F<sub>ed</sub></b>
1	10.421	1.340	2.169	68.697	1.564
2	10.420	1.389	2.247	65.138	1.573
3	10.420	1.387	2.252	65.938	1.577
4	10.416	1.371	2.202	65.080	1.560
5	10.417	1.373	2.208	65.203	1.563
6	10.419	1.374	2.249	68.327	1.585
7	10.418	1.369	2.172	63.099	1.545
8	10.4203	1.390	2.257	65.690	1.577
9	10.420	1.353	2.178	66.788	1.560
10	10.420	1.357	2.176	65.767	1.556

In the above table, values of hole diameter, diameter of delamination, area of hole, and area of delamination are extracted from the module. Further using the equation 3, delamination factor is calculated. As delamination factor is the most vital criteria to determine hole quality, the values of delamination factor for each of the hole is compared with each other. In the analysis, the focus is towards the comparison of these three factors:  $F_d$ ,  $F_{da}$ ,  $F_{ed}$ , and its dependant variables. Using Microsoft Excel to calculate and picturize the extracted data, comparison is conducted.

By taking delamination area into consideration, a clear view on delamination between each hole can be obtained. By plotting a chart with obtained delamination area values, calculating average of obtained values, and interpolating the values, a reasonable justification can be provided for the behavior and variations in the values.

## **4.2. Analysis of delamination**

From the Figure 10 (a) for the cutting parameters, cutting speed  $v_c$  100 mm/rev and feed 0.02 mm/rev it is evident the delamination increases with respect to number of holes drilled. The delamination increases gradually from 60 to 70 mm<sup>2</sup>. Generally, the delamination area is increased on 15% which is not significant, however, this is mainly caused due to the tool wear that takes place over usage [40]. The relatively high delamination area for the very first hole, when the drill bit was fresh, indicates to inappropriate

---

cutting data for current drill geometry, since the fresh drill, in theory, must provide the minimum of defects. The difference between the delamination of the 1<sup>st</sup> and the 160<sup>th</sup> drilled hole can be visually seen in Figure 11. The delamination contour has been recognized using the image processing algorithms described in Chapter 2. For the cutting parameters,  $v_c$  100 m/min and feed 0.05 mm/rev, we can see that the delamination area initially drops down for certain holes, this can be caused because of the increase in temperature at the interface of tool and hole which reacts with the metal matrix of the composite, which results in softening of the metal matrix, which gradually reduces the delamination. But, once tool wear starts to act, again we can see an increase in delamination towards the end. For the cutting parameters, as shown in Figure 10 (c),  $v_c$  100 mm/rev and feed 0.15 mm/rev, we can identify that, the trend of the delamination area gradually increases with number of holes. The delamination area ranges from 55 to 60 mm<sup>2</sup>. Even though the degree is lower, significance of comparison is higher. The gradual increase in delamination area is because of the increase in tool wear, thrust force and temperature induced due to friction that affect the matrix and tool's cutting edge. For the cutting parameters, as shown in Figure 10 (d),  $v_c$  100 mm/rev and feed 0.1 mm/rev, the delamination factor increases with increase in number of drilled holes. The range of the delamination area lies between 50 to 65 mm<sup>2</sup>. The change in delamination area is mainly caused because of the wear in the tool generated during the continuous drilling process.

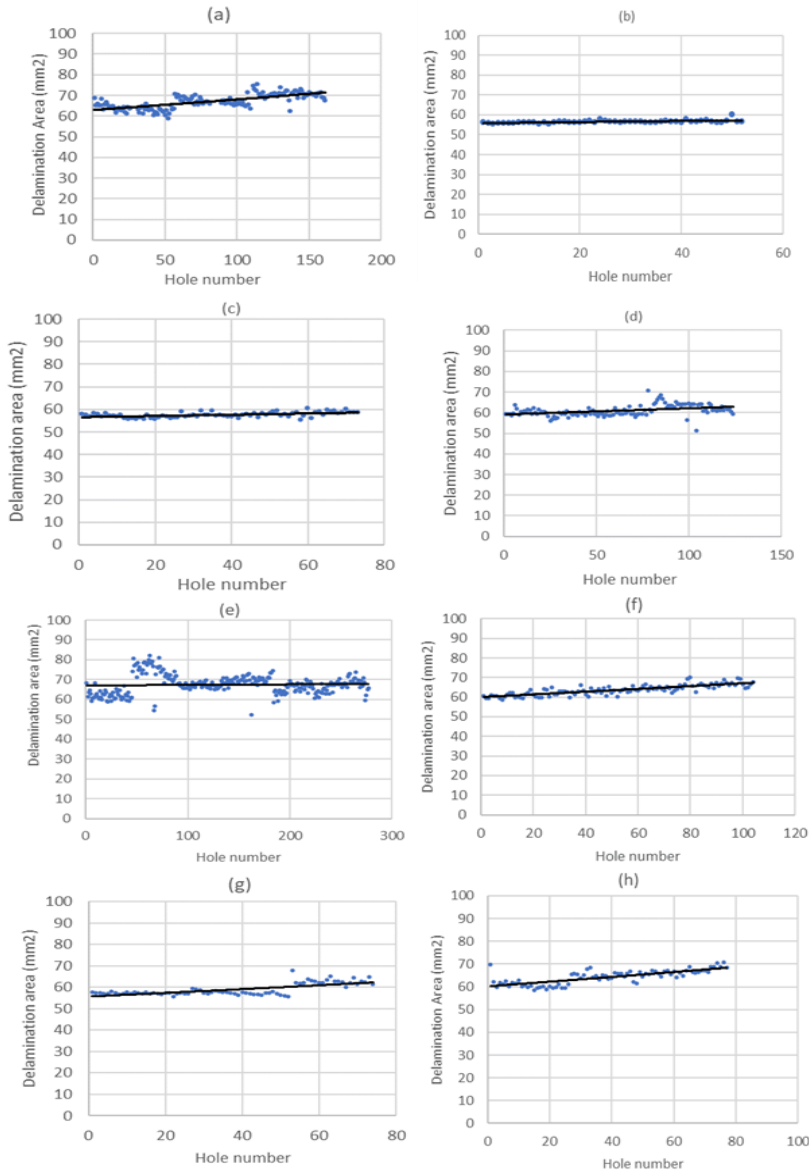


**Figure 10:** Comparison of Delamination area for different cutting data a)  $vc=100$  mm/rev;  $f=0.02$  mm/rev b)  $vc=100$  m/min;  $f=0.05$  mm/rev c)  $vc=100$  m/min;  $f=0.15$  mm/rev d)  $vc=100$  m/min;  $f=0.1$  mm/rev e)  $vc=140$  m/min;  $f=0.02$  mm/rev f)  $vc=140$  m/min;  $f=0.1$  mm/rev g)  $vc=180$  m/min;  $f=0.05$  mm/rev h)  $vc=180$  m/min;  $f=0.15$  mm/rev



---

For the cutting parameters, as shown in Figure 10 (e),  $v_c$  140 m/min and feed 0.02 mm/rev we can deduce that the trendline increases with increase in number of holes drilled, but with very low degree. This is mainly because of the tool wear caused due to continuous drilling process. The range of the delamination area is between 60 to 70 mm<sup>2</sup>, with few irregular values of delamination area, which may be caused because of improper cutting conditions. For the cutting parameters, as shown in Figure 10 (f),  $v_c$  140 m/min and feed 0.1 mm/rev, we can observe that the trendline increases with increase in number of holes drilled linearly. This is mainly because of the tool wear caused due to continuous drilling process and the thermal damage. The range of the delamination area is between 60 to 70 mm<sup>2</sup>, with few irregular values of delamination area, which may be caused because of improper cutting conditions. For the cutting parameters, as shown in Figure 10 (g),  $v_c$  180 m/min and feed 0.05 mm/rev we could see that delamination area gradually increases with respect to the number of drilled holes. During the initial phase of the drilling process, the delamination area tends to be minimal when compared to the later part of drilling process. This behavior is because of the thermal damage caused during the drilling process and tool deterioration. The lowest value of delamination area recorded in this is graph was 56 mm<sup>2</sup> at the first hole. Whereas, towards the final phase of drilled holes, the delamination area range was observed to be 62 mm<sup>2</sup>. The Variation between the first and final drilled hole was around 6 mm<sup>2</sup>. For the cutting parameters, as shown in Figure 10 (h),  $v_c$  180 m/min and feed 0.15 mm/rev, we could observe that the delamination area trend is linear concerning the number of drilled holes. During the first hole of the drilling process, the delamination area tends to be minimal compared to the later part of the drilling process. The Delamination area has been gradually increasing with the number of drilled holes. This behavior is because of the thermal damage caused during the drilling process and tool deterioration. The lowest value of delamination area recorded in this is graph was 60 mm<sup>2</sup> at the first hole. Whereas, towards the final phase of drilled holes, the delamination area range was observed to be around 70 mm<sup>2</sup>. The difference between the first and last drilled hole was about 10 mm<sup>2</sup>. We could observe a similar trend for all the cutting conditions. Also, the range of delamination area is observed to be 60 to 70 mm<sup>2</sup>. Comparatively, the cutting conditions with  $v_c$  100 m/min, feed 0.15 mm/rev and  $v_c$  100 m/min, feed 0.05 mm/rev have exhibited a lower delamination area range. Whereas the following cutting conditions have exhibited higher signs of delamination area:  $v_c$  100 m/min, feed 0.02 mm/rev;  $v_c$  180 m/min, feed 0.15 mm/rev and  $v_c$  140 m/min, feed 0.1 mm/rev. So, the major reason for the fluctuation in the delamination area is

---

the increase in thrust force due to the increase in feed and the thermal damage due to the continuous drilling process.

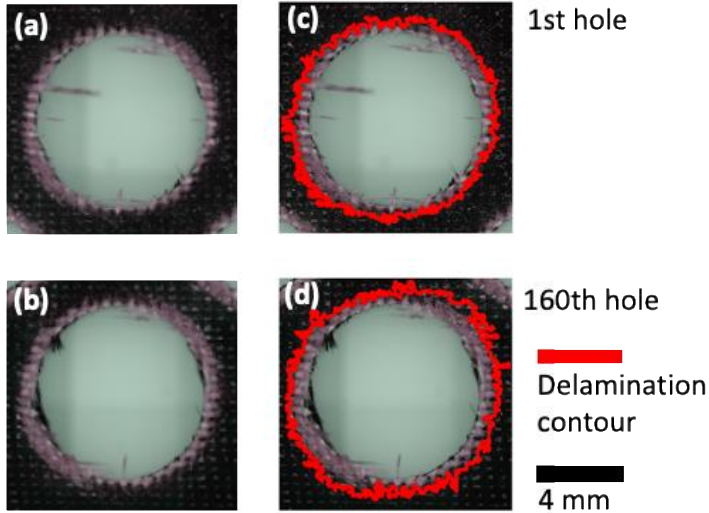


**Figure 11.** Drilled holes using cemented carbide drill with  $v_c$  100 m/min,  $f$  0.02 mm/rev, (a) the 1<sup>st</sup> drilled hole and (b) is 160<sup>th</sup> drilled holes, (c,d) are holes with recognized delamination contours

In the above figure, the hole quality is compared between the 1<sup>st</sup> and 160<sup>th</sup> hole using the delamination contour. We could observe the drastic difference in delamination area highlighted by contour between the 1<sup>st</sup> hole and 160<sup>th</sup> hole. This difference is caused mainly due to the tool wear because of continuous drilling process. Both delamination area and uncut fiber area shows a drastic change, comparatively. Continue analysing the hole quality for  $v_c = 100$  m/min and  $f = 0.02$  mm/rev, various delamination criteria such as  $F_d$ ,  $F_{da}$ ,  $F_{ed}$  by Equations 1, 3, 4 have been calculated for following drilled holes. The plot of these criteria can be seen in Figure 11.

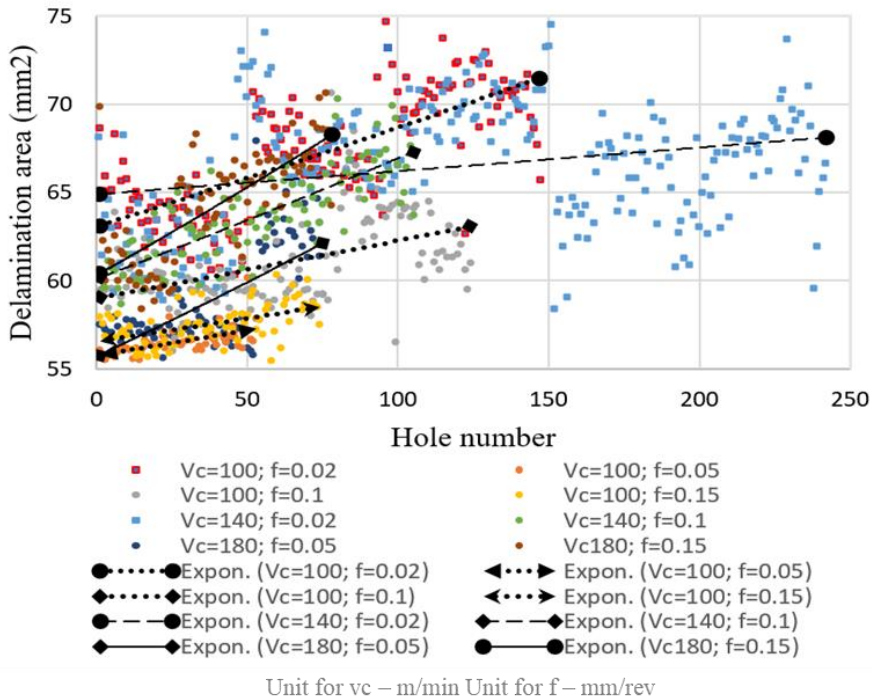


**Figure 12:** Comparison chart of delamination area for all cutting data

The above figure shows the behavior and change in delamination area for all the cutting data over number of holes drilled. From the image it is evident that for  $vc=180$ ; the delamination area is comparatively lower than  $vc=100$  and  $vc=140$ . By comparing different feed rate for identical cutting speed, we can identify that delamination area increases with increase in feed rate. The delamination area gradually increases from 60 to 70 mm<sup>2</sup> range for feed rate 0.15 and cutting speed 180. But for feed rate 0.05, the delamination area gradually increases from 55 to 65 mm<sup>2</sup>, which is significantly lower compared to higher feed rate. But for lower cutting speeds, the delamination area is higher. This is mainly caused due to thrust force created during the drilling process. By comparing different feed rate for cutting speed 100 rpm, we can identify that delamination area decreases with increase in feed rate. As thrust force is directly dependent on cutting speed and feed rate, thrust force is usually higher for lower cutting speed and lower feed rate. And the temperature generated between the cutting tool and workpiece interface will be comparatively lower than higher cutting speed, thus the smoothing factor of matrix material is lower in low cutting speeds. Thus, from the

analysis, we can identify that for lower cutting speed, the higher the feed rate, the delamination area is lower, whereas, with higher cutting speed, lower the feed rate, the delamination area is comparatively lower.

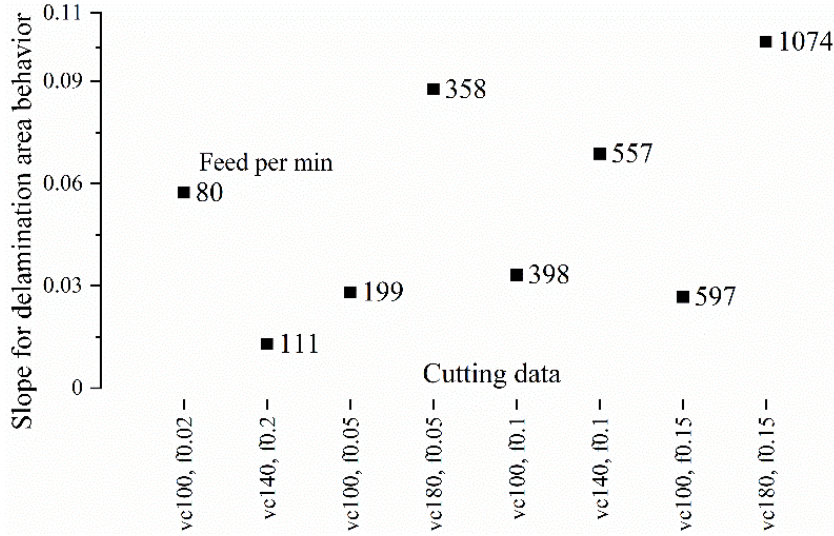


**Figure 13:** Slope values for each cutting data

The above figure (Figure 13) shows the values of slope of delamination area behavior for each of the cutting data. When compared with each other, the cutting data  $vc=180$  m/min and  $f=0.15$  mm/rev, has the higher value of slope. This indicated that the tool performance is the least for the respective cutting condition. The most ideal cutting data for tool performance is for cutting speed  $vc=140$  m/min and  $f=0.2$  mm/rev. The cutting data,  $vc=100$  m/min;  $f=0.05$  mm/rev,  $vc=100$  m/min;  $f=0.15$  mm/rev, has almost identical values of slope, which indicated that the behavior of these cutting conditions is similar. As the slope is calculated with ratio of feed per min, the change in slope for each of the cutting data gives us a clear comparison on tool performance for each of the cutting data.

## Analysis of delamination factor

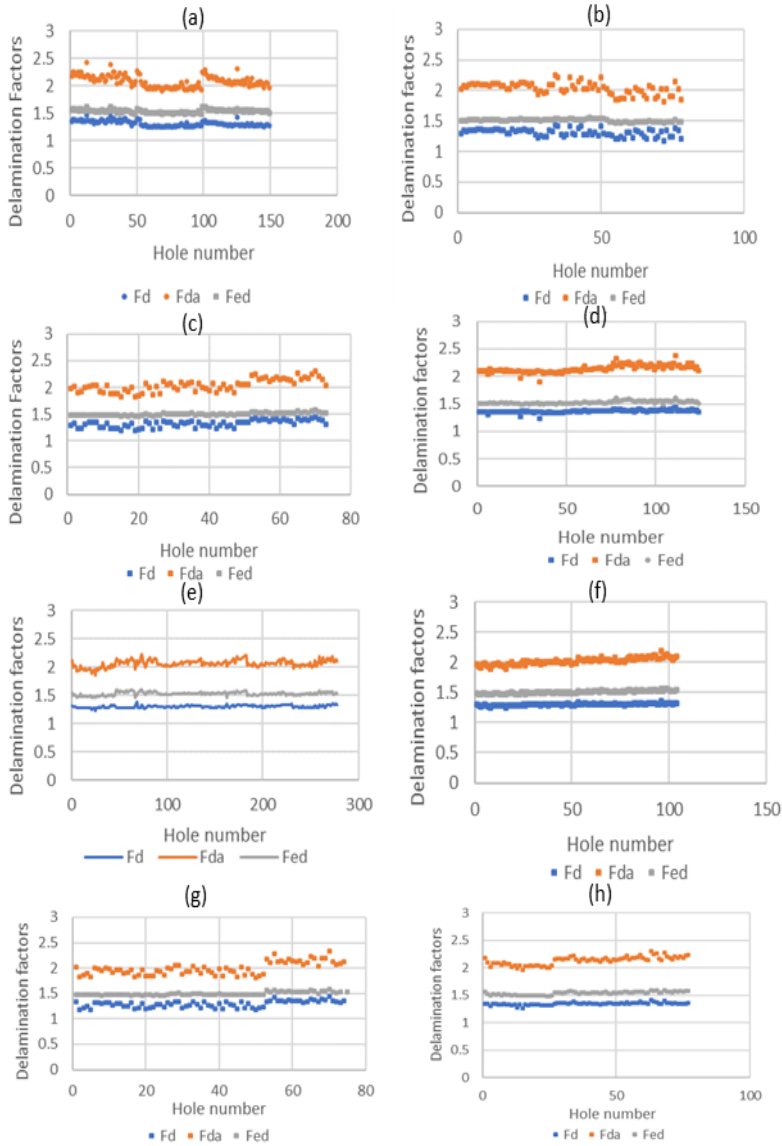


**Figure 14:** Delamination factors for different cutting data; a)  $vc=100$  m/min;  $f=0.02$  mm/rev b)  $vc=100$  m/min;  $f=0.05$  mm/rev c)  $vc=100$  m/min;  $f=0.15$  mm/rev d)  $vc=100$  m/min;  $f=0.1$  mm/rev e)  $vc=140$  m/min;  $f=0.02$  mm/rev f)  $vc=140$  m/min;  $f=0.1$  mm/rev g)  $vc=180$  m/min;  $f=0.05$  mm/rev h)  $vc=180$  m/min;  $f=0.15$  mm/rev

---

For the cutting parameters,  $v_c$  100 m/min and feed 0.02 mm/rev, we can conclude that all delamination factors behave similarly. If we compare the values of delamination factor  $F_d$  and adjusted delamination factor  $F_{da}$ , the behavior is very similar despite on higher amplitude of  $F_{da}$ . But, for equivalent delamination factor  $F_{ed}$ , compared to  $F_d$  and  $F_{da}$ , the behavior is varying to a very small degree. This is because of the irregular delamination that takes place between the holes and  $F_{ed}$  takes both area and diameter of delamination into consideration. Therefore,  $F_{ed}$  compensates the size deviation of the delamination ( $D_{max}$ ) and delamination area that barely neglects the shape changes of the delamination. While  $F_d$  completely depends on delamination maximum diameter  $D_{max}$  considering every little spike, and  $F_{da}$  even enhances this behavior including the area dependency,  $F_{ed}$  smooths by compensating  $D_{max}$  and area by each other. Thus,  $F_{ed}$  can be used for hole series which have high variation of the size and shape, while  $F_d$  and  $F_{da}$  characterizes the delamination more detailed showing every little changes of delamination size and shape. For the cutting parameters,  $v_c$  100 m/min and feed 0.05 mm/rev, we can identify that the behavior of all delamination factors is similar. Even though the  $F_{da}$  amplitude is comparatively higher than  $F_d$  and  $F_{ed}$ , the trend of the data is evidently similar. The equivalent delamination factor is much more accurate because of irregular delamination that takes place during the drilling process. Thus, the trend of  $F_{ed}$  is comparatively linear than  $F_{da}$  and  $F_d$ . For the cutting parameters,  $v_c$  100 m/min and feed 0.15 mm/rev, the behavior of  $F_d$  and  $F_{ad}$  is quite similar. But, for  $F_{ed}$ , the trend is comparatively linear than  $F_d$  and  $F_{ad}$ . This is because,  $F_{ed}$  takes both  $D_{max}$ , and delamination area into consideration according to equation 4. The rate of change of delamination factor, throughout the process proceeds at almost a constant rate which gives us the insight that the cutting conditions are more adequate for the process. For the cutting parameters,  $v_c$  100 m/min and feed 0.1 mm/rev, we can see that behavior of  $F_d$  and  $F_{da}$  is quite identical, with only change in amplitude. The amplitude of  $F_{da}$  is higher than  $F_d$  and  $F_{ed}$ , comparatively.  $F_{ed}$  trendline shows that the delamination factor higher towards the end, which denotes that delamination factor increases with increase in number of drilled holes. For the cutting parameters,  $v_c$  140 m/min and feed 0.02 mm/rev, we can see that behavior of  $F_d$  and  $F_{ed}$  is quite identical, with only change in amplitude. The amplitude of  $F_{da}$  is higher than  $F_d$  and  $F_{ed}$ , comparatively. The trendline shows that the delamination factor higher towards the end, which denotes that delamination factor increases with increase in number of drilled holes. For the cutting parameters,  $v_c$  140 m/min and feed 0.1 mm/rev, we can see that behavior of  $F_d$  and  $F_{ed}$  is quite identical, with only change in amplitude. The amplitude of  $F_{da}$  is higher than  $F_d$  and  $F_{ed}$ , comparatively. The trendline of  $F_{da}$

---

shows that the delamination factor higher towards the end, which denotes that delamination factor increases with increase in number of drilled holes. For the cutting parameters,  $vc$  180 m/min and feed 0.05 mm/rev, we can see that behavior of  $F_d$  and  $F_{da}$  is quite identical, with only change in amplitude. The amplitude of  $F_{da}$  is higher than  $F_d$  and  $F_{cd}$ , comparatively. The trendline of  $F_{da}$  shows that the delamination factor higher towards the end, which denotes that delamination factor increases with increase in number of drilled holes. For the cutting parameters,  $vc$  180 m/min and feed 0.15 mm/rev, we can see that behavior of  $F_d$  and  $F_{cd}$  is quite identical, with only change in amplitude. The amplitude of  $F_{da}$  is higher than  $F_d$  and  $F_{cd}$ , comparatively. The trendline of  $F_{da}$  shows that the delamination factor higher towards the end, which denotes that delamination factor increases with increase in number of drilled holes.

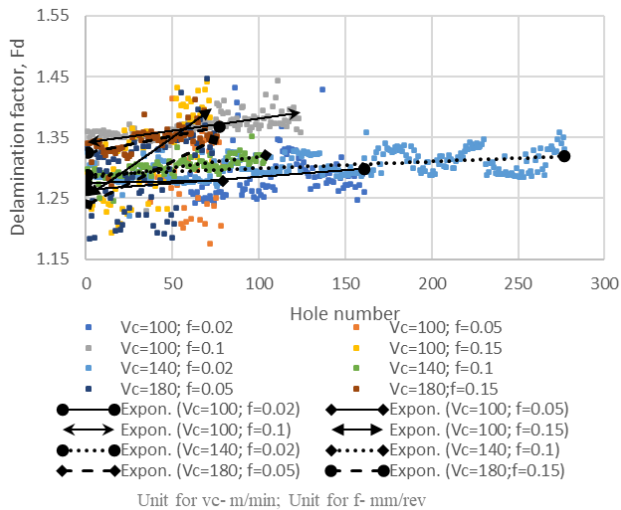


**Figure 15:** Comparison chart for delamination factor  $F_d$

From the overall comparison of delamination factor, we could see that cutting conditions,  $vc$  100 m/min,  $f$  0.15mm/rev and  $vc$  140 m/min,  $f$  0.1mm/rev exhibits inclined trend. Whereas the rest of the cutting conditions have indicated slightly linear behavior.  $vc$  100 m/min,  $f$  0.1mm/rev and  $vc$  140 m/min,  $f$  0.02mm/rev have the highest delamination factor range from 1.3 to 1.4.  $vc$  100 m/min,  $f$  0.02mm/rev and  $vc$  180 m/min,  $f$  0.05mm/rev indicates lower range of delamination factor i.e., 1.24 to 1.35.

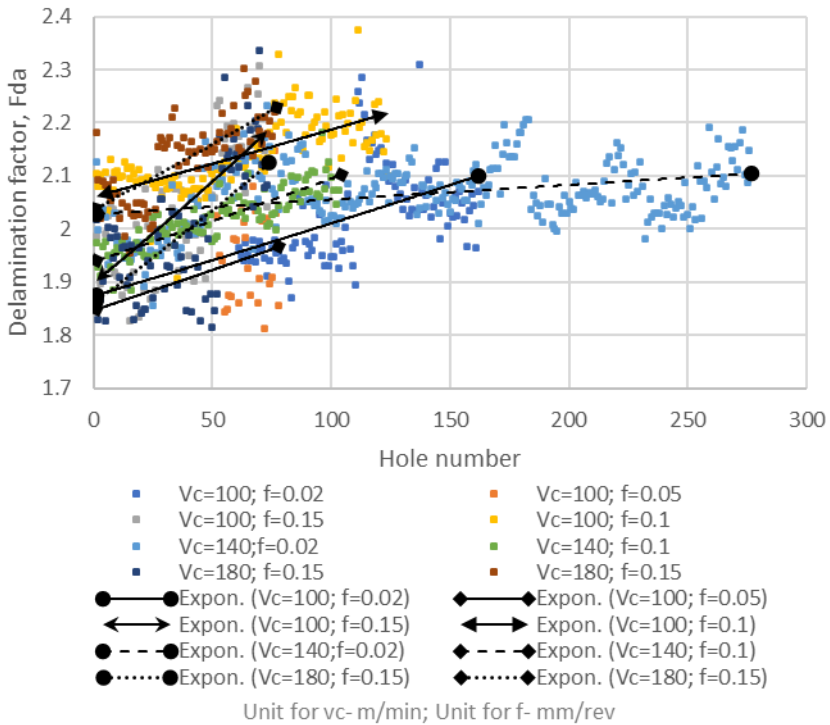


**Figure 16:** Comparison chart for adjusted delamination factor,  $F_{da}$

From the overall comparison of adjusted delamination factor, we could see that cutting conditions, except  $vc$  140 m/min,  $f$  0.02mm/rev, have exhibited inclined trend. Whereas  $vc$  140 m/min,  $f$  0.02mm/rev have indicated slightly linear behavior.  $vc$  180 m/min,  $f$  0.15mm/rev and  $vc$  100 m/min,  $f$  0.1mm/rev have the highest delamination factor range from 2 to 2.25.  $vc$  100 m/min,  $f$  0.05mm/rev and  $vc$  100 m/min,  $f$  0.02mm/rev indicates lower range of delamination factor i.e., 1.85 to 2.



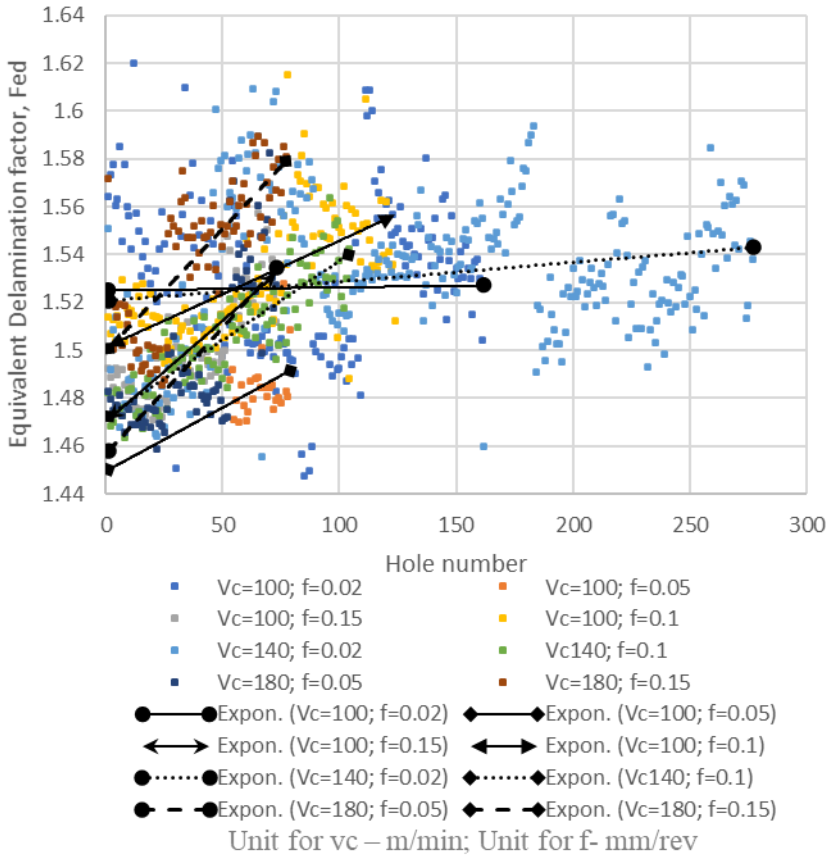


**Figure 17:** Comparison chart for Equivalent delamination factor  $F_{ed}$ .

From the overall comparison of equivalent delamination factor, we could see that cutting conditions, except  $v_c$  140 m/min,  $f$  0.02mm/rev and  $v_c$  100 m/min,  $f$  0.02mm/rev, have exhibited inclined trend. Whereas  $v_c$  140 m/min,  $f$  0.02mm/rev and  $v_c$  100 m/min,  $f$  0.02mm/rev, have indicated slightly linear behavior.

The cutting data  $v_c$  100 m/min,  $f$  0.1mm/rev and  $v_c$  180 m/min,  $f$  0.15mm/rev have the highest delamination factor range from 1.5 to 1.58.  $v_c$  100 m/min,  $f$  0.05mm/rev;  $v_c$  180 m/min,  $f$  0.05mm/rev and  $v_c$  100 m/min,  $f$  0.15mm/rev indicates lower range of delamination factor i.e., 1.45 to 1.52.

---

**PCD drill: For cutting speed 140 m/min and feed= 0.1 mm/rev**

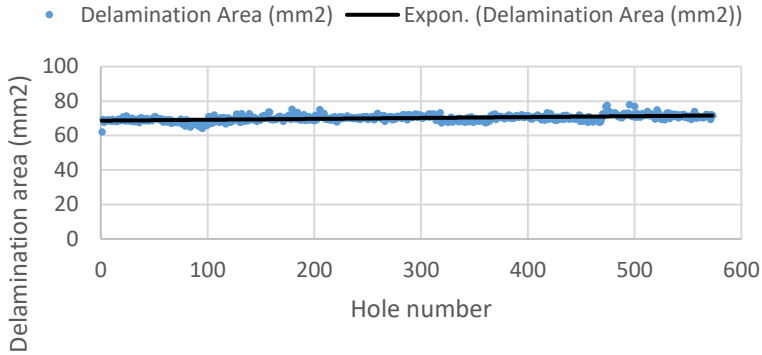


**Figure 18:** Delamination area for PCD coated tool

From the above figure, the delamination factor increases gradually with increase in number of drilled holes. The range of the delamination area lies between 70 to 73 mm<sup>2</sup>. The delamination area enlargement is caused by the tool deterioration and heat generated by the drilling process.

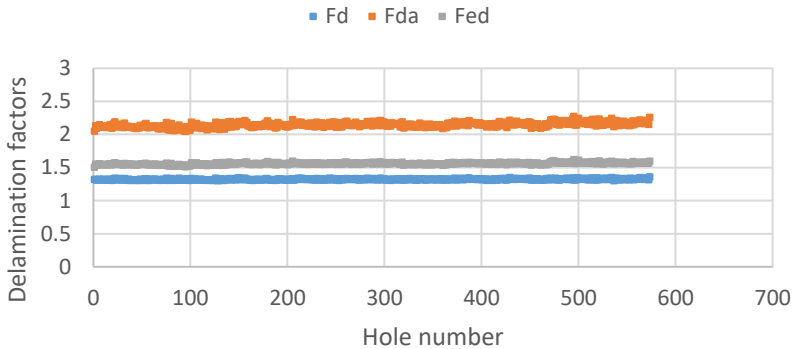


**Figure 19:** Delamination factor chart for PCD coated tool

From the above figure, we can deduce that, the behavior of delamination factor with respect to hole number is almost identical for all the three factors of delamination. When compared with each other, F<sub>da</sub> shows a higher magnitude than F<sub>ed</sub> and F<sub>d</sub>. Ranging from 2.1 to 2.3, with a steady inclination, it is quite evident to extract few key information about tool wear. With around 580 holes drilled with the same tool and same cutting data, this analysis gives us a clear picture on how tool wear affects the delamination factor and other criteria.

### 4.3. Analysis of uncut fiber area

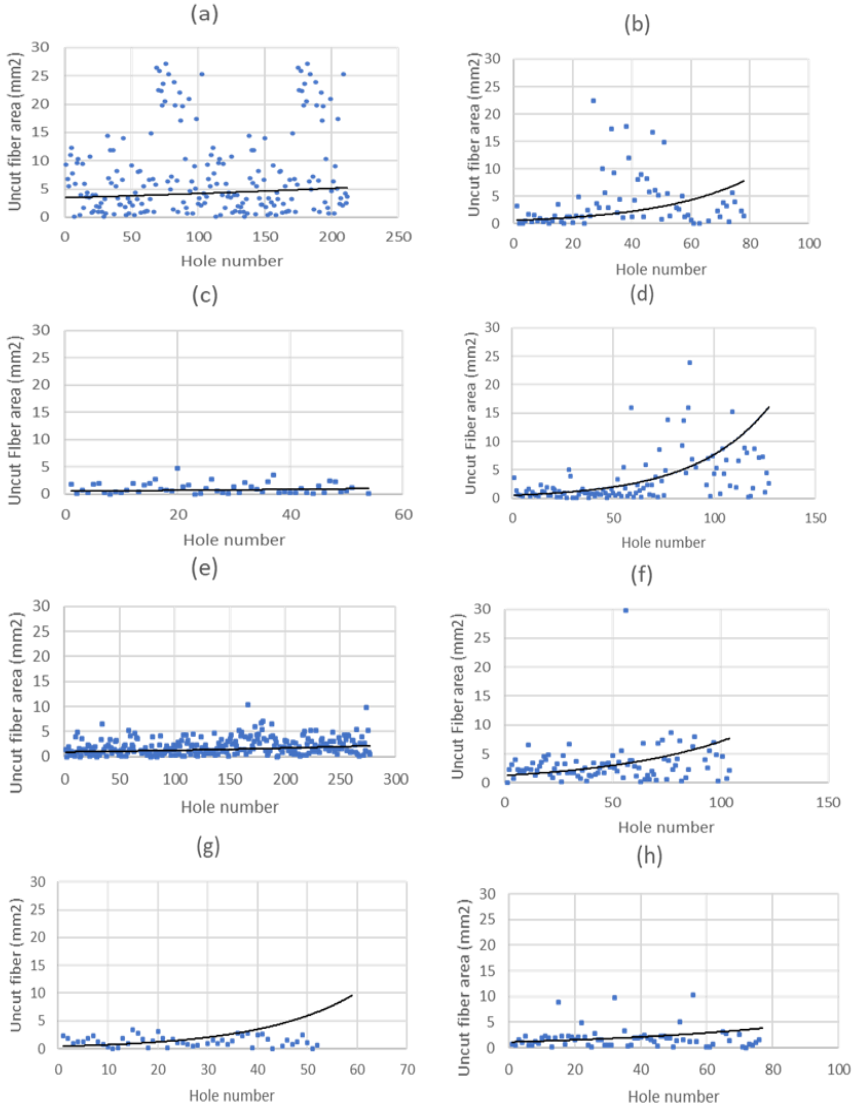


**Figure 20:** Combined chart for uncut fiber area for different cutting data  
 a)  $vc=100$  m/min;  $f=0.02$  mm/rev b)  $vc=100$  m/min;  $f=0.05$  mm/rev c)  
 $vc=100$  m/min;  $f=0.15$  mm/rev d)  $vc=100$  m/min;  $f=0.1$  mm/rev e)  $vc=140$   
 $m/min$ ;  $f=0.02$  mm/rev f)  $vc=140$  m/min;  $f=0.1$  mm/rev g)  $vc=180$  m/min;  
 $f=0.05$  mm/rev h)  $vc=180$  m/min;  $f=0.15$  mm/rev

---

From the above figure, it evident that the behavior of change in area of uncut fiber with respect to hole number is almost similar for all the cutting data. Although, the range of uncut fiber area is almost same for all the data, it is crucial to identify even the smallest variations that take place within. The gradual increase of uncut fiber area is mainly caused due to the tool wear induced due to continuous operation and contact zone of cutting edge and workpiece. Gradually when operation continues due to increase in thrust force, the trendline shows the inclined behavior. Through overall comparison we can identify that for  $v_c=140$  m/min and  $f=0.02$  mm/rev, the range of uncut fiber area is lower, comparatively. When comparing for single cutting speed and varying feed rate, we can identify that for lower feed rate, uncut fiber area is comparatively lower. For instance, for feed rate 0.02 mm/rev, and cutting speed 100 m/min, the value of uncut fiber area is 4mm<sup>2</sup> to 5mm<sup>2</sup>. But, for higher feed rates, like  $f=0.1$  mm/rev, the uncut fiber area is adequately higher when compared to lower feed rates. Even though the value of slope for all the plots seems similar, there are adequate change in slopes for certain cutting data like  $v_c=100$  m/min, and  $f=0.1$  mm/rev and  $v_c=180$  m/min and  $f=0.05$  mm/rev. From the above figure, it is also evident that the trend of the slope increases towards the later part of the drilling process or towards the last few holes drilled in the panel. The increase in uncut fiber area towards the last few holes denotes the tool wear that influences the hole quality.

When the values of uncut fiber area for each cutting data are compared, for  $v_c=100$  m/min and  $f=0.02$  mm/rev, the values range from 4 to 6 mm<sup>2</sup>, for  $v_c=100$  m/min,  $f=0.05$  mm/rev, values range from 1 to 7 mm<sup>2</sup>, with most of the data focused under 5 mm<sup>2</sup>. For  $v_c=100$  m/min and  $f=0.15$  mm/rev, the range is very low compared to all other cutting conditions, ranging from 1 to 2 mm<sup>2</sup>. For  $v_c=140$  m/min and  $f=0.02$  mm/rev, the range is quite low comparatively. For  $v_c=180$  m/min, both the trendline shows that the value of area is higher towards the later part of the panel.

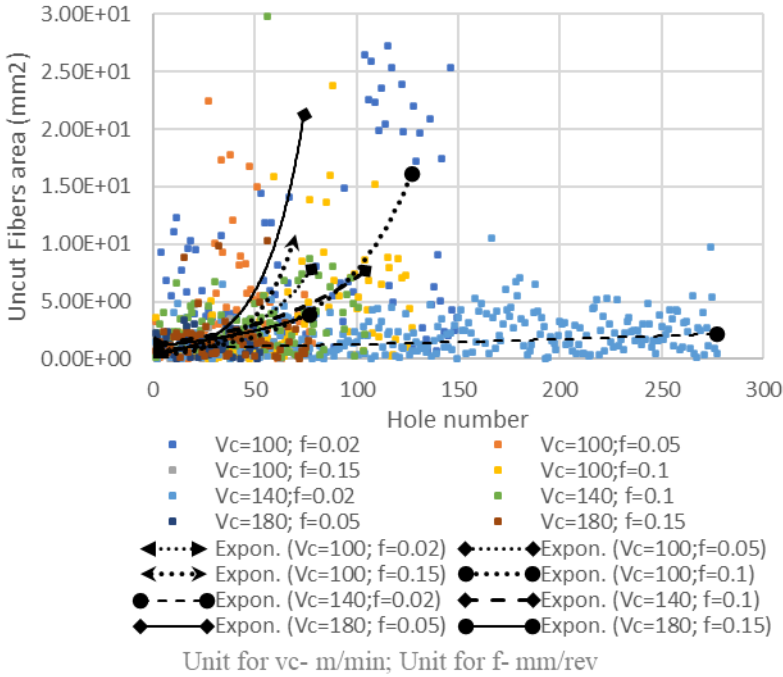


**Figure 21:** Comparison chart for uncut fiber area

From the figure, the comparison chart clearly shows the difference between each of the values and behavior of uncut fiber areas for different cutting data. Through overall comparison, we can identify that, the trendline behavior is almost identical for  $v_c=180$  m/min with  $f=0.05$  mm/rev and  $v_c=100$  m/min with  $f=0.1$  mm/rev, with a higher value of slope. The trendline for  $v_c=140$  m/min and  $f=0.02$  mm/rev, is almost linear, which shows the operation is steady throughout the panel and with good cutting conditions. As an overall comparison, it is identifiable that the uncut fiber values come under  $10\text{mm}^2$ . Few spikes are also noted in the data, which may be caused due to the improper cutting conditions and overlapping caused during image processing.

---

### 4.3.1. PCD uncut fibers

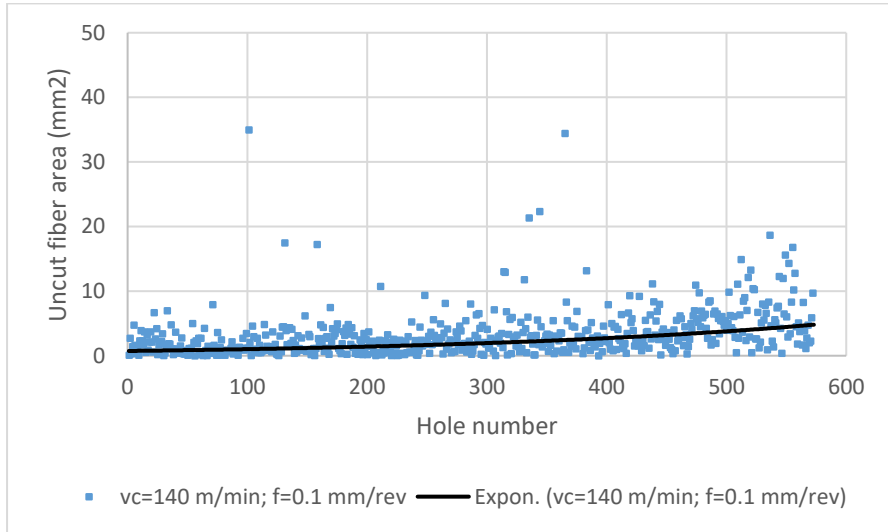


**Figure 22:** *Uncut fiber area chart for PCD drill*

The above figure (Figure 22) shows that behavior of uncut fiber area for drilled holes using PCD tool. From the chart, it is evident that the tool performance for the cutting data used is comparatively better than CC tool. Even though the uncut fiber area for PCD range from 0 to 10mm<sup>2</sup>, the number of holes ratio for PCD to CC is quite high. With nearly 600 holes drilled for PCD, the behavior shows promising tool performance, comparatively. So, it is possible to conclude that PCD tool has better performance for optimal cutting data than CC tool.

---

## 5. Discussion and Conclusion

A thorough literature review was conducted to identify all the important factors and variables that can affect the hole quality. As a comparative study, it is crucial to identify even the slightest of factors that could have an effect the hole quality to provide a clear overview on the analyzed data. From the reliable sources and similar studies conducted on the topic, it was identified that the main factors that affect the hole quality of a drilled hole for a CFRP material are delamination and uncut fibers. The defects in drilling process are mainly caused due to tool wear and thrust force induced during the drilling process. Further, focusing individually on delamination and uncut fibers, the main variables that takes effect are identified as maximum delamination diameter, delamination area and uncut fiber area. Then, the factors that determine the delamination that occurs in the hole is identified as delamination factor, adjusted delamination factor and equivalent factor. The equations that were used to calculate these identified factors are given in Equation 1,2 and 4. To achieve these values for the factors, image processing and microscopy is identified as the key processes. During the analysis process, over 80 panels were analyzed with drilled holes, varying from 20 to 30 holes per panel. Table 1 shows the different cutting data used for drilling the holes and the number of holes drilled for each cutting data. Two type of drill bits were used for drilling the holes, a drill bit with CC coated and another with PCD coated. With various cutting speed and feed rate, each hole provided various data that can be analyzed and compared.

For analysis of panels, high-quality images are expected to get more accurate results. Alicona infinite focus microscope was used to scan the CFRP panels and to get images with high resolutions. All the panels were focused and scanned under the microscope carefully with 2.5x lens to get the details in the holes. From the obtained images through microscopy, all the images were input in MATLAB with special scripts to run a module to identify the center of the drilled hole. Delamination area contours, uncut fiber contours were identified from the module as output data. Using this module, the values of uncut fiber area, delamination area, maximum delamination diameter, delamination factor  $F_d$ , adjusted delamination factor  $F_{da}$ , and equivalent delamination factor  $F_{ed}$  is obtained. The methodology is mainly based on six modules that are used in a sequential order. They are: (i) defining the circumference of the hole, (ii) defining the contours of the uncut fibers, (iii) defining the delaminated area, (iv) creating and analysing the profiles of uncut fibers, (v) creating and analysing the profiles of delamination, and (vi) estimating a general evaluation of hole quality.

---

With almost 1600 values of all the data, data management plays a vital role in comparison of all the data. This is achieved by identifying and segregating the values for different cutting data. After scaling and converting all the obtained to a uniform unit, picturization of data is carried out. This is achieved by plotting graphs with each factor taken at y axis with respect to hole number on the x axis. To see the clear picture on the behavior and change in values, each data is initially plotted individually and studied thoroughly. After plotting the graphs, the irregularities were identified within the plots. Few of the data were beyond the range and easily identified as overlapping caused during image processing. These data were carefully identified and segregated from the actual data to get a more reliable and logical outcome. With the hole diameter with 7.8 mm, the maximum uncut fiber area can be maximum of 30 mm<sup>2</sup>, thus the values or spikes beyond 30mm<sup>2</sup> were neglected from the actual data. Using the scatter plot to show the quantity of data analysed and using exponential interpolation scheme to represent the behavior of the defects, a clear picture on the change in delamination and uncut fibers is achieved.

From the results obtained, we can conclude that for higher cutting speed and lower feed rate the range of the delamination area is much lower compared to lower cutting speed, as per figure 20. But, for lower cutting speed, the higher the feed rate the delamination area tends to be lower, up 15%. Even though change remains to be at 15% for all the varying parameters, it is significant when it comes to comparison point of view. The steady inclination in delamination area and uncut fiber area from 1<sup>st</sup> hole to the last hole, indicated that tool wear comes into action during the drilling process. The main reason for the delamination and uncut fiber being thrust force and tool wear, it is logical to conclude that during the process, with increase in number of holes drilled, the results obtained are as expected. The delamination factors  $F_d$ ,  $F_{da}$  and  $F_{ed}$ , are the variables that determine the actual hole quality. From the results obtained, the trendline shown in the figure 24, indicated that the delamination factor also increases with increase in number of drilled holes, as maximum delamination diameter is directly proportional to delamination factor. Even though, the change is below 0.05, this comparative study clearly gives the necessary information about each cutting condition. A similar trend also takes into action for  $F_{da}$  and  $F_{ed}$ , but with a higher magnitude because, both  $F_{da}$  and  $F_{ed}$  takes both area of delamination and maximum delamination diameter into consideration, whereas  $F_d$  focuses only on maximum delamination diameter. The irregularity in the diameter is one of the major reasons where  $F_{ed}$  is the factor that is more accurate. Finally, as an overall conclusion it is evident to propose



---

using the comparative study conducted, that for cutting speed  $v_c=100, 140$  and  $180$  m/min, the results show promising quality of the holes. When compared to each other, the study shows that for higher cutting speed, the lower the feed rate, the delamination factor and uncut fibers tend to be lower. Whereas, for lower cutting speed, fluctuations are found within the range of delamination and uncut fibers, sliding slightly towards higher feed rate.

As an overall conclusion, based on the evidence collected, we can conclude that, for the optimal cutting conditions and cutting data, PCD tool has better performance than CC tool for CFRP drilling. PCD has shown a very high performance – slope of delamination area was  $0.01$ . The cutting data  $v_c=140$  m/min  $f=0.02$  mm/rev, can be identified as the best cutting data to be used for CFRP drilling, but we always aim to have the highest drilling performance (material removal ration), thus we increased the feed for PCD to  $0.1$ .

From the overall results obtained, and along with similar literature and theory, the results are quite adequate and compliments the outcome from this comparative study. So, it is not understated to conclude that the results obtained, and the comparison provided are reliable.

---

## 6. References

- [1] H. Hocheng, *Machining technology for composite materials: Principles and practice*. 2011.
- [2] G. Bakis *et al.*, “Mechanical properties of the carbon nanotube modified epoxy–carbon fiber unidirectional prepreg laminates,” *Polymers (Basel)*, vol. 13, no. 5, pp. 1–14, 2021, doi: 10.3390/polym13050770.
- [3] G. B. V. Kumar and R. Pramod, “Investigation of mechanical properties of aluminium reinforced glass fibre polymer composites,” *AIP Conf. Proc.*, vol. 1859, 2017, doi: 10.1063/1.4990237.
- [4] M. M. A. Nassar, R. Arunachalam, and K. I. Alzebeleh, “Machinability of natural fiber reinforced composites: a review,” *Int. J. Adv. Manuf. Technol.*, vol. 88, no. 9–12, pp. 2985–3004, 2017, doi: 10.1007/s00170-016-9010-9.
- [5] T. Zhao, Q. Zhao, W. Wu, L. Xi, Y. Li, and Z. Wan, “Enhancing weld attributes in ultrasonic spot welding of carbon fibre-reinforced thermoplastic composites : Effect of sonotrode configurations and process control,” vol. 211, no. September 2020, 2021, doi: 10.1016/j.compositesb.2021.108648.
- [6] L. Chen, M. Li, X. Yang, and B. Li, “Thermal defect characterization and heat conduction modeling during fiber laser cutting carbon fiber reinforced polymer laminates,” *Arch. Civ. Mech. Eng.*, vol. 20, no. 2, pp. 1–14, 2020, doi: 10.1007/s43452-020-00064-8.
- [7] J. Nyaporo, M. A. Ahmed, H. El-hofy, and M. El-hofy, “Fluid-structure interaction modeling of the abrasive waterjet drilling of carbon fiber reinforced polymers,” *J. Manuf. Process.*, vol. 58, no. September 2019, pp. 551–562, 2020, doi: 10.1016/j.jmapro.2020.08.035.
- [8] X. Li, X. Ruan, J. Zou, X. Long, and Z. Chen, “Experiment on carbon fiber – reinforced plastic cutting by abrasive waterjet with specific emphasis on surface morphology,” pp. 145–156, 2020.
- [9] Z. Li, D. Zhang, W. Qin, and D. Geng, “Removal analyses of chip and rod in rotary ultrasonic-assisted drilling of carbon fiber-reinforced plastics using core drill,” no. 37, 2016, doi: 10.1177/0731684416644510.
- [10] H. Khayyam, R. N. Jazar, S. Nunna, and G. Golkarnarenji, “Progress in Materials Science PAN precursor fabrication , applications and thermal stabilization process in carbon fiber production : Experimental and mathematical modelling,” *Prog. Mater. Sci.*, vol. 107, no. June 2019, p. 100575, 2020, doi: 10.1016/j.pmatsci.2019.100575.
- [11] M. Li, S. Li, X. Yang, Y. Zhang, and Z. Liang, “Effect of lay-up configuration and processing parameters on surface quality during fiber laser cutting of CFRP laminates,” *Int. J. Adv. Manuf. Technol.*, vol. 100, no. 1–4, pp. 623–635, 2019, doi: 10.1007/s00170-018-2728-9.
- [12] R. Badrnezhad and R. Eslami-farsani, “Modeling and Differential Evolution Optimization of PAN Carbon Fiber Production Process,” vol. 15, no. 6, pp. 1182–1189, 2014, doi: 10.1007/s12221-014-1182-z.
- [13] M. A. Karatas, “A review on machinability of carbon fi ber reinforced polymer ( CFRP ) and glass fi ber reinforced polymer ( GFRP ) composite

- 
- materials,” vol. 14, pp. 318–326, 2018, doi: 10.1016/j.dt.2018.02.001.
- [14] J. Kumar and R. K. Verma, “Experimental investigation for machinability aspects of graphene oxide / carbon fiber reinforced polymer nanocomposites and predictive modeling using hybrid approach,” *Def. Technol.*, no. xxxx, 2020, doi: 10.1016/j.dt.2020.09.009.
- [15] S. Vigneshwaran, M. Uthayakumar, and V. Arumugaprabu, “Review on Machinability of Fiber Reinforced Polymers: A Drilling Approach,” *Silicon*, vol. 10, no. 5, pp. 2295–2305, 2018, doi: 10.1007/s12633-018-9764-9.
- [16] S. Å. H. Johansson and G. C. R. Ossbahr, “A Study of the Influence of Drilling Method and Hole Quality on Static Strength and Fatigue Life of Carbon Fiber Reinforced Plastic Aircraft Material,” no. 724, 2018.
- [17] C. M. Machado, D. Silva, and C. Vidal, “A new approach to assess delamination in drilling carbon fibre-reinforced epoxy composite materials,” pp. 3389–3398, 2021.
- [18] A. Najiah, H. Ascroft, and S. Barnes, “Materials Today : Proceedings An investigation of hole quality during drilling of carbon fibre reinforced plastic and titanium ( Ti6Al4V ) using tungsten carbide drills,” *Mater. Today Proc.*, vol. 29, no. November 2018, pp. 161–167, 2020, doi: 10.1016/j.matpr.2020.05.640.
- [19] I. M. Hakimi, S. Sharif, and D. Kurniawan, “Laminate Orientation Effect on Drilling of Carbon Fiber Reinforced Plastic Composites,” *Appl. Mech. Mater.*, vol. 315, pp. 768–772, 2013, doi: 10.4028/www.scientific.net/AMM.315.768.
- [20] “Drill terminology and cutting characteristics.” [http://www.mitsubishicarbide.com/en/technical\\_information/tec\\_rotating\\_tools/drills/tec\\_drills\\_technical\\_top/tec\\_drilling\\_terminology](http://www.mitsubishicarbide.com/en/technical_information/tec_rotating_tools/drills/tec_drills_technical_top/tec_drilling_terminology).
- [21] S. C. (Firm), *Modern Metal Cutting: A Practical Handbook*. Sandvik Coromant, 1994.
- [22] Z. Jia, C. Chen, F. Wang, C. Zhang, and Q. Wang, “Analytical model for delamination of CFRP during drilling of CFRP / metal stacks,” pp. 5099–5109, 2020.
- [23] Z. Jia, C. Chen, F. Wang, and C. Zhang, “Analytical study of delamination damage and delamination-free drilling method of CFRP composite,” *J. Mater. Process. Tech.*, vol. 282, no. December 2019, p. 116665, 2020, doi: 10.1016/j.jmatprotec.2020.116665.
- [24] C. L. Tan and A. I. Azmi, “Analytical study of critical thrust force for on-set delamination damage of drilling hybrid carbon / glass composite,” pp. 929–941, 2017, doi: 10.1007/s00170-017-0152-1.
- [25] J. Saoudi, R. Zitoune, and S. Gururaja, “Analytical and experimental investigation of the delamination during drilling of composite structures with core drill made of diamond grits : X-ray tomography analysis,” 2017, doi: 10.1177/0021998317724591.
- [26] L. V. Pinho, D. Carou, and J. P. Davim, “Comparative study of the performance of diamond-coated drills on the delamination in drilling of carbon fiber reinforced plastics : assessing the influence of the temperature
-

- 
- of the drill,” 2015, doi: 10.1177/0021998315571973.
- [27] A. Hrechuk, V. Bushlya, and J. E. Ståhl, “Hole-quality evaluation in drilling fiber-reinforced composites,” *Compos. Struct.*, vol. 204, no. June, pp. 378–387, 2018, doi: 10.1016/j.compstruct.2018.07.105.
- [28] A. Hrechuk, V. Bushlya, R. M’Saoubi, and J. E. Ståhl, “Experimental investigations into tool wear of drilling CFRP,” *Procedia Manuf.*, vol. 25, pp. 294–301, 2018, doi: 10.1016/j.promfg.2018.06.086.
- [29] J. P. Davim, J. C. Rubio, and A. M. Abrao, “A novel approach based on digital image analysis to evaluate the delamination factor after drilling composite laminates,” *Compos. Sci. Technol.*, vol. 67, no. 9, pp. 1939–1945, 2007, doi: 10.1016/j.compscitech.2006.10.009.
- [30] D. A. Sandoval, J. J. Roa, O. Ther, E. Tarrés, and L. Llanes, “Micromechanical properties of WC-(W,Ti,Ta,Nb)C-Co composites,” *J. Alloys Compd.*, vol. 777, pp. 593–601, 2019, doi: 10.1016/j.jallcom.2018.11.001.
- [31] J. García, V. Collado Ciprés, A. Blomqvist, and B. Kaplan, “Cemented carbide microstructures: a review,” *International Journal of Refractory Metals and Hard Materials*, vol. 80. Elsevier Ltd, pp. 40–68, Apr. 01, 2019, doi: 10.1016/j.ijrmhm.2018.12.004.
- [32] G. Li, M. Z. Rahim, W. Pan, C. Wen, and S. Ding, “The manufacturing and the application of polycrystalline diamond tools – A comprehensive review,” *J. Manuf. Process.*, vol. 56, no. May, pp. 400–416, 2020, doi: 10.1016/j.jmapro.2020.05.010.
- [33] D. A. Stephenson and J. S. Agapiou, *Metal Cutting Theory and Practice, Third Edition*. 2016.
- [34] A. Hrechuk, D. Johansson, V. Bushlya, L. Devin, and J. E. Ståhl, “Application of Colding tool life equation on the drilling fiber reinforcement polymers,” *Procedia Manuf.*, vol. 25, pp. 302–308, 2018, doi: 10.1016/j.promfg.2018.06.087.
- [35] D. A. Macdonald, “The application of focus variation microscopy for lithic use-wear quantification,” *J. Archaeol. Sci.*, vol. 48, no. 1, pp. 26–33, 2014, doi: 10.1016/j.jas.2013.10.003.
- [36] “Alicona Infinite focus.”  
<https://www.alicona.com/en/products/infinitefocus/>.
- [37] M. Wolfram, “Moore neighbourhood.”  
<https://mathworld.wolfram.com/MooreNeighborhood.html>.
- [38] Delaunay, “Delaunay Triangulation.”  
[https://mathworld.wolfram.com/DelaunayTriangulation.html#:~:text=The Delaunay triangulation is a,94\)](https://mathworld.wolfram.com/DelaunayTriangulation.html#:~:text=The Delaunay triangulation is a,94)).
- [39] “Least Square Method.”  
<https://mathworld.wolfram.com/LeastSquaresFitting.html>.
- [40] E. Rahim, T. Ogawa, A. Miura, H. Sasahara, R. Koyasu, and Y. Yao, “A novel approach to evaluate the delamination factor of CFRP hole,” *Proc. 6th Int. Conf. Lead. Edge Manuf. 21st Century, LEM 2011*, 2011, doi: 10.1299/jsmelem.2011.6\_3417-1\_.
-

---

## 7. APPENDIX

